APL Materials

# Progress and prospects in the quantum anomalous Hall effect

Cite as: APL Mater. **10**, 090903 (2022); https://doi.org/10.1063/5.0100989
Submitted: 27 May 2022 • Accepted: 23 August 2022 • Published Online: 20 September 2022

Hang Chi and Jagadeesh S. Moodera

APL Materials PERSPECTIVE scitation.org/journal/apm

# Progress and prospects in the quantum anomalous Hall effect

Cite as: APL Mater. 10, 090903 (2022); doi: 10.1063/5.0100989
Submitted: 27 May 2022 • Accepted: 23 August 2022 •
Published Online: 20 September 2022



Hang Chi[1,2,a)] and Jagadeesh S. Moodera[1,3,b)]

## AFFILIATIONS

[1] Francis Bitter Magnet Laboratory, Plasma Science and Fusion Center, Massachusetts Institute of Technology, Cambridge, Massachusetts 02139, USA
[2] U.S. Army CCDC Army Research Laboratory, Adelphi, Maryland 20783, USA
[3] Department of Physics, Massachusetts Institute of Technology, Cambridge, Massachusetts 02139, USA

**Note:** This paper is part of the Special Topic on Materials Challenges and Synthesis Science of Emerging Quantum Materials.
[a)] **Author to whom correspondence should be addressed:** chihang@mit.edu
[b)] **Email:** moodera@mit.edu

## ABSTRACT

The quantum anomalous Hall effect refers to the quantization of the Hall effect in the absence of an applied magnetic field. The quantum anomalous Hall effect is of topological nature and well suited for field-free resistance metrology and low-power information processing utilizing dissipationless chiral edge transport. In this Perspective, we provide an overview of the recent achievements as well as the material challenges and opportunities, pertaining to engineering intrinsic/interfacial magnetic coupling, that are expected to propel future development in this field.



## I. INTRODUCTION

The quantum anomalous Hall (QAH) effect represents one of the triumphs in conceptualizing topological aspects of electronic states in condensed matter physics.[1–11] It constitutes an ever-evolving family of Hall effects.[12] In 1879, Edwin Herbert Hall discovered that the Lorentz force leads to a transverse voltage when the longitudinal current in a conductor is subjected to a perpendicular external magnetic field[13]—an effect that bears his name and inspires researchers to push the scientific and technological frontiers.[14] This ordinary Hall (OH) effect offers a direct tool in assessing the charge carrier type and density in semiconductors, as well as acts as a practical probe in measuring the magnetic field. Hall later reported an unusual and stronger response in ferromagnets with qualitatively different field dependence.[15] It hence came to be known as the anomalous Hall (AH) effect, correlated with the spontaneous magnetization $M$. Its deep roots in topology and geometry were appreciated in recent times,[16] enabled by the discoveries of integer[17] and fractional[18,19] quantum Hall (QH) effects in the 1980s.

For a two-dimensional electron gas (2DEG) under strong applied magnetic field, the Hall resistance $R_{yx}$ develops well-defined plateaus, quantized to exact value of $h/\nu e^2$ at which the longitudinal resistance $R_{xx}$ vanishes. Here, $h$ is Planck's constant, $e$ is the elementary charge, and $\nu$ is the filling factor that is topological in nature and corresponds to the Chern numbers (by integrating the Berry curvature[20] over the first Brillouin zone) summed over the occupied bands. In the integer QH regime, the quasi-1D chiral edge channels, each contributing a quantized Hall conductance $G_{xy} = e^2/h$, are immune to back scattering. For practical utilization of such dissipationless edge transport, e.g., in resistance metrology and low-energy-cost electronics, it is natural to desire a QAH system displaying a quantized version of the AH effect. It allows QH states to prevail at zero magnetic field, circumventing the necessity of forming Landau levels as well as the often stringent requirement on sample mobility.[21–23]

It became clear that, similar to the QH physics, the intrinsic AH conductivity $\sigma_{AH}$ in a magnetic material is governed by the integral of the Berry curvature over occupied bands.[24–29] Effort toward realizing the QAH effect was nonetheless at an impasse for decades, as $\sigma_{AH}$ is not quantized in metals with partially occupied bands and magnetic insulators with a non-zero Chern number are rare to come by. Since around 2005, however, new prospects emerged

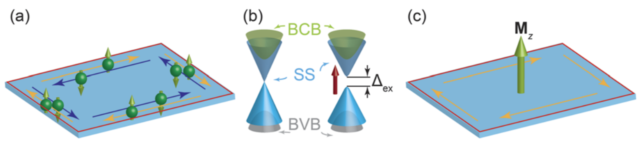


**FIG. 1.** Quantum anomalous Hall effect with exchange gap opening in topological insulator film. (a) The helical edge conduction in 2D TI protected by the time-reversal symmetry (TRS), displaying the quantum spin Hall effect. (b) Left, bulk conduction (BCB) and valence (BVB) bands of a typical 3D TI, along with the gapless surface states (SSs) protected by the TRS. Right, an exchange gap $\Delta_{ex}$ induced in the SSs through broken TRS. (c) The chiral edge states in the quantum anomalous Hall effect with spontaneous perpendicular magnetization $\mathbf{M}_z$ in magnetic TI. No external magnetic field is required for the dissipationless chiral edge current.

accompanying the discovery of topological insulators (TIs) with strong spin–orbit coupling (SOC) under the protection of time-reversal symmetry (TRS).[30,31] As shown in Fig. 1(a), a 2D TI characterized by a single $Z_2$ topological invariant hosts a pair of spin-polarized helical edge states (can be roughly understood as two copies of the chiral QH states with opposite spin[32]) that leads to the quantum spin Hall (QSH) effect with quantized six-terminal $R_{xx}$ of $h/2e^2$ and transverse spin-accumulation.[33–39]

Upon generalizing to 3D,[40] as exemplified by the $Bi_2Te_3$ family of materials,[41–44] TI features insulating bulk and gapless helical surface states (SSs) with Dirac-like linear dispersion and spin-momentum locking, see Fig. 1(b). Introducing magnetic order to break the TRS in 2D TI, will intuitively lead to a QAH state—when one spin block is driven out of the topologically nontrivial band inverted regime into the normal one with vanishing $G_{xy}$.[45] Despite early progress, this route was not pursued further, largely owing to the finite magnetic field needed to induce quantization as a result of the paramagnetic nature of Mn doping in HgTe.[46] As shown in Fig. 1(c), an alternative platform was brought forth to leverage 3D TI thin films instead, where each 2D SS of 3D TI contributes a half-quantized $G_{xy} = \pm e^2/2h$ under broken TRS.[47–49] In 2013, this was realized in Cr-doped ternary $(Bi,Sb)_2Te_3$ thin films,[50] soon gaining wide acceptance with ideal performance.[51–61] More recently, the QAH effect was also demonstrated in one device of five-layer exfoliated intrinsic antiferromagnetic TI $MnBi_2Te_4$,[62] as well as in Moiré materials, namely, magic-angle twisted bilayer graphene[63] and AB-stacked $MoTe_2/WSe_2$ heterostructures,[64] greatly expanding the available material platforms and physical mechanisms for investigating the QAH phenomena.

## II. REALIZING THE QAH EFFECT

As shown in Fig. 2(a), the archetypical 3D TI of the $Bi_2Te_3$-based materials crystallize in a $R\bar{3}m$ ($D^5_{3d}$, No. 166) rhombohedral structure, featuring Te(1)–Bi–Te(2)–Bi–Te(1)-type quintuple layers (QLs) with weak van der Waals interlayer bonding.[65–67] The topologically nontrivial members of the family display a single surface Dirac cone[41] and bandgap of 0.2–0.33, 0.21–0.3, and 0.13–0.2 eV, for $Bi_2Se_3$,[68–70] $Sb_2Te_3$,[68,71,72] and $Bi_2Te_3$,[68,71,73–75] respectively. The chemical stoichiometry and prevalence of defects sensitively affect the transport properties.[76] When grown as thin films using molecular beam epitaxy (MBE), $Bi_2Se_3$ and $Bi_2Te_3$ are chiefly $n$ type, owing to Se and Te vacancies, while $Sb_2Te_3$ is dominantly $p$ type due to $Sb_{Te}$ antisite defects. The isostructural nature of the compounds and availability of different carrier types offer the needed tunability for adjusting the chemical potential to zero-in on the surface transport.

Development of diluted magnetic semiconductors in the early 2000s has provided important insights into the induction of long-range magnetic order in TIs. Taking $Sb_2Te_3$ for example, Mn doping in $Mn_xSb_{2-x}Te_3$ bulk crystals does not stimulate long-range ordering for $x$ up to 0.045,[77] although ferromagnetism can be stabilized in $Mn_xBi_{2-x}Te_3$ ($x$ up to 0.09)[78] as well as in topological crystalline insulator $Mn_xSn_{1-x}Te$ ($x$ up to 0.12).[79] Doping with V and Cr, on the other hand, is effective in introducing magnetic order in $V_xSb_{2-x}Te_3$ ($0.01 \le x \le 0.03$)[80] and $Cr_xSb_{2-x}Te_3$ ($x$ up to 0.095).[81] With the incorporation of magnetic dopants (V/Cr)

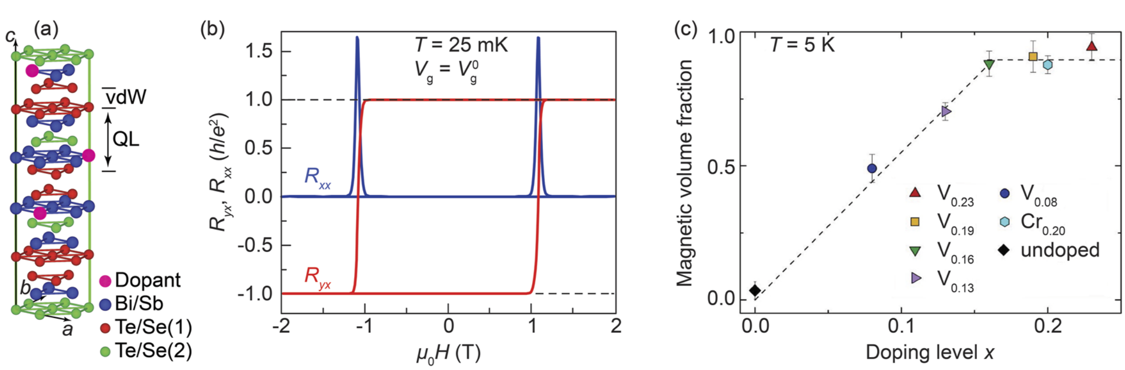


**FIG. 2.** Quantum anomalous Hall effect in magnetically doped topolgoical insulator films. (a) The crystal structure of $(Bi,Sb)_2(Te,Se)_3$ featuring quintuple layers (QLs) interconnected by weak van der Waals (vdW) bonding. Magnetic transition metal dopant V, Cr or Mn can occupy the Bi/Sb site and induce long range magnetic ordering (while any dopant occupation in between layers would not be favorable). (b) The QAH state realized at the charge neutrality point in a 4 QL thick $V_{0.11}(Bi_{0.29}Sb_{0.71})_{1.89}Te_3$ film at 25 mK. (c) The magnetic volume fraction measured by low energy muon spin rotation (LE-$\mu$SR) technique, as a function of the doping level $x$ in $(V,Cr)_x(Bi,Sb)_{2-x}Te_3$. Adapted with permission from Chang *et al.*, Nat. Mater. **14**, 473–477 (2015). Copyright 2015 Springer Nature Limited, (b); Adapted with permission from Krieger *et al.*, Phys. Rev. B **96**, 184402 (2017). Copyright 2017 American Physical Society, (c).

elevated to even higher levels in the out-of-equilibrium MBE growth, strong out-of-plane ferromagnetic ordering has been successfully demonstrated with Curie temperature $T_C$ reaching 177 and 190 K in $V_xSb_{2-x}Te_3$ ($x$ up to 0.35)[82] and $Cr_xSb_{2-x}Te_3$ ($x$ up to 0.59),[83] respectively. These early works on relatively thick films (hundreds of nm) have benchmarked the solubility limit, while setting expectation of the achievable exchange energy in films with thickness relevant to the QAH effect, considering that $T_C$ generally decreases upon reducing the thickness.[84] The high doping, however, is expected to weaken and eventually destroy the topological nature of the band due to reduced SOC. At an intermediate level, $V_xSb_{2-x}Te_3$ ($x$ up to 0.10) thin films can sustain high surface mobility, leading to the prominent Shubnikov–de Haas (SdH) quantum oscillations.[85]

Despite its larger bandgap and more ideally positioned surface Dirac cone, the ferromagnetic response from Cr-doped $Bi_2Se_3$ is quite weak.[86] The effort toward realizing the QAH effect has since largely been focused on the ternary $(Bi,Sb)_2Te_3$ matrix, with systematically engineered thickness and Bi/Sb alloying ratio. The QAH state was first demonstrated by Cr doping in 5 QL $Cr_{0.15}(Bi_{0.1}Sb_{0.9})_{1.85}Te_3$.[50] It was then discovered that V doping instead leads to a better reproducibility and a more robust QAH effect.[56] As shown in Fig. 2(b), a nearly ideal QAH state is present at the charge neutrality point in 4 QL $V_{0.11}(Bi_{0.29}Sb_{0.71})_{1.89}Te_3$, manifesting zero magnetic field $R_{yx}(0) = 1.000\,19 \pm 0.000\,69\ h/e^2$, $R_{xx}(0) = 0.000\,13 \pm 0.000\,07\ h/e^2$ and an AH angle $\alpha$ of $89.993° \pm 0.004°$ at 25 mK. As revealed by low energy muon spin rotation (LE-$\mu$SR) spectroscopy in Fig. 2(c), the full magnetic volume fraction is achieved in $(Cr,V)_x(Bi,Sb)_{2-x}Te_3$ only at doping levels with $x \geq 0.16$. The evolution of the effective magnetic ordering is consistent with the formation and growth of ferromagnetic islands that eventually encompass full volume upon cooling.[87]

The edge current–voltage $I_i = (e^2/h)\sum_j (T_{ji}V_i - T_{ij}V_j)$, is determined by the transmission probability $T_{ji}$, connecting the $i$th electrode to the $j$th electrode in the Landauer–Büttiker theory.[88,89] As shown in Figs. 1(c) and 3, in the QAH regime, the chiral edge modes propagate clockwise (counter-clockwise) for $M > 0$ ($M < 0$), leading to $T_{i,i+1} = 1$ ($T_{i+1,i} = 1$). The ideal dissipationless chiral edge transport at zero magnetic field has indeed been verified by comprehensive local and nonlocal magnetoresistance experiments.[52,90–92] In quantum phase transitions concerning a QAH insulator, the temperature dependence of the derivative of $R_{xx}(H)$ at the critical field $H_c$ follows a power law scaling behavior $(dR_{xx}/dH)|_{Hc} \propto T^{-\kappa}$, with critical exponent $\kappa$ in the range 0.22–0.62.[93–97] Utilizing a cryogenic current comparator, metrologically comprehensive low-current, high-precision measurements of the QAH states have demonstrated $R_{yx}$ quantization within 1 part per million (ppm) of the von-Klitzing constant $R_K$,[98–100] and most recently down to 10 parts per billion (ppb), leveraging a permanent magnet design.[101] It improves the prospects for zero-field quantum resistance standard and spintronics exploiting chiral edge transport, which favors a more robust QAH state at higher temperature, with even smaller $R_{xx}$ and larger breakdown current density.[102,103]

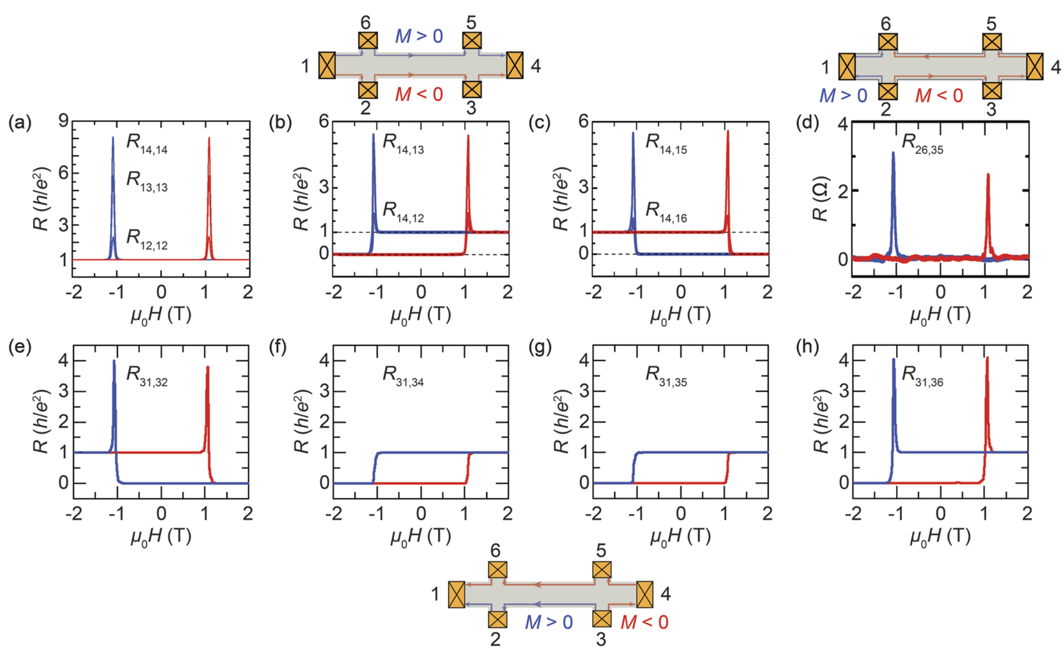


**FIG. 3.** Local and nonlocal transport in the quantum anomalous Hall regime. Magnetic field $\mu_0H$ dependence at $T = 25$ mK for (a) two-terminal resistances $R_{12,12}$, $R_{13,13}$, $R_{14,14}$; three-terminal resistances (b) $R_{14,13}$, $R_{14,12}$; (c) $R_{14,15}$, $R_{14,16}$; (d) nonlocal resistance $R_{26,35}$; and additional three-terminal measurements (e) $R_{31,32}$; (f) $R_{31,34}$; (g) $R_{31,35}$; (h) $R_{31,36}$. The first (last) two subscripts in the resistance notation refer to the current (voltage) leads. The chiral current flows are depicted in the device schematics as insets: top left for (a)–(c), top right for (d) and bottom for (e)–(h). The red and blue lines indicate the chiral edge current for magnetization into ($M < 0$) and out of the plane ($M > 0$), respectively. Adapted with permission from Chang *et al.*, Phys. Rev. Lett. **115**, 057206 (2015). Copyright 2015 American Physical Society.

## III. HIGHER TEMPERATURE QAH EFFECT

In early QAH studies, the critical temperature $T_{\rm QAH}$ reaching full quantization is rather low in the mK range. By Cr/V codoping, the $T_{\rm QAH}$ can be enhanced to 0.3 K with $R_{yx}(0) = h/e^2$ (within the experimental uncertainty) and $R_{xx}(0) = 0.009\ h/e^2$, while at $T = 1.5$ K, $R_{yx}(0) = 0.97\ h/e^2$ and $R_{xx}(0) = 0.19\ h/e^2$.[104] The increase in the $T_{\rm QAH}$ via Cr/V codoping verifies to have originated from the improved magnetic homogeneity and favorably modulated surface band structure.

Further increase in the $T_{\rm QAH}$ would be beneficial in order to advance quantitative understanding of the QAH physics and to facilitate practical applications. There are apparent disadvantages in introducing ferromagnetic order via traditional doping though: (i) the foreign species act as defects that inevitably degrade the sample quality; (ii) the innate random distribution of magnetic dopants leads to undesirable disorder (including spin scattering) and fluctuation in the energy band (in addition to the more generic local variations of the Bi/Sb ratio and/or film thickness) that adversely affect the QAH state;[105–109] (iii) at the high level of doping, or rather substitution, needed for enhanced $T_C$, the band structure is prone to the development of impurity states in the bulk gap and its topological nature may also be affected, let alone the likelihood of secondary phase segregation.[110] Thus, unfortunately, the doping route comes with inherent limitations.

The challenging yet highly desirable goal of raising the $T_{\rm QAH}$ is being actively pursued. A successful approach involves magnetic modulation doping. Specifically, as shown in Fig. 4(a), apart from the conventional single-layer $Cr_x(Bi,Sb)_{2-x}Te_3$ with uniform and modest Cr doping ($x = 0.10$), alternating combinations of heavily doped ($x = 0.46$) and pristine ($x = 0$) TI QLs are rationally designed to form tri- or penta-layer stacks. The penta-layer structure enables an impressively high $T_{\rm QAH} = 0.5$ K, while $R_{yx}(0)$ reaches $0.97\ h/e^2$ at 2 K, as shown in Fig. 4(b).[111] The greatly suppressed disorder and magnetic fluctuation are believed to be the key in enhancing the $T_{\rm QAH}$. In the modulation doping case, as we shall see below, there is also the possibility that the internal interfacial exchange interaction becomes highly effective, leading to a better exchange gap opening in the "cleaner/pristine" layers of TI, thus enabling the achievement of a higher $T_{\rm QAH}$.

It is worth pointing out that, at such high level of Cr substitution on the Bi/Sb sites (exceeding 20%), the SOC is expected to be much weakened, and the band inversion may no longer sustain. It hence drives the Cr-rich layer away from the TI phase toward a magnetic insulator (MI) instead. The versatility of the MI-like heavily Cr-doped TI block has been recognized and extended to an architecture of [3 QL $Cr:(Bi,Sb)_2Te_3$/4 QL $(Bi,Sb)_2Te_3]_n$/3 QL $Cr:(Bi,Sb)_2Te_3$.[112] Similar to an earlier TI-normal insulator design of [6 QL $(Cr,V):(Bi,Sb)_2Te_3$/3.5 nm $CdSe]_n$/6 QL $(Cr,V):(Bi,Sb)_2Te_3$ multilayers,[113] it successfully facilitates the demonstration of the high Chern number (adjustable by the stacking number $n$) QAH state.[114,115] This design also allows for probing the physics underlying the plateau-to-plateau phase transition connecting the Chern number $C = 1$ and $C = 2$ phases, by means of systematically engineering the strength of SOC, via tuning the Cr concentration, in the middle Cr-doped layer of a penta-layer device.[116] The Chern number tunable QAH state attests to the capability and precise control of multichannel dissipationless chiral conduction. Recently, as illustrated in Fig. 4(c), asymmetric placement of the Cr-rich block in a semi-magnetic configuration allows selective opening of an exchange gap only in the top surface of TI.[117] It enables condensed matter investigation of the relativistic parity anomaly in quantum field theory, offering long-sought experimental verification of the half-integer quantization of $G_{xy}$ in Fig. 4(d).

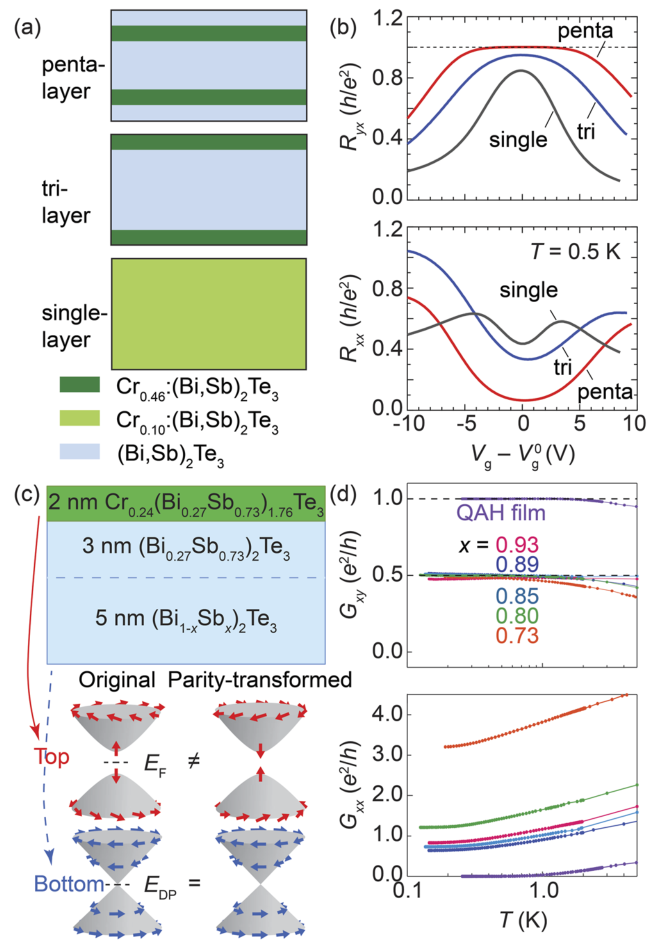


**FIG. 4.** Magnetic modulation doping for higher quantization temperature and parity anomaly. (a) Schematics of lightly doped uniform single-layer (bottom), modulation-doped tri- (middle) and penta-layer (top) by alternating heavily Cr-doped and undoped $(Bi,Sb)_2Te_3$. (b) The gate dependence of the Hall resistance $R_{yx}$ and longitudinal resistance $R_{xx}$ measured at 0.5 K in the absence of magnetic field. (c) Schematics of asymmetric magnetic TIs with gapped top and gapless bottom surface Dirac states, enabling condensed matter investigation of relativistic parity anomaly. (d) Half-integer quantization of the zero-field Hall conductance $G_{xy}$ and the accompanying sheet conductance $G_{xx}$. Adapted with permission from Mogi *et al.*, Appl. Phys. Lett. **107**, 182401 (2015). Copyright 2015 AIP Publishing, [(a) and (b)]; Adapted with permission from Mogi *et al.*, Nat. Phys. **18**, 390–394 (2022). Copyright 2022 Springer Nature Limited, [(c) and (d)].

## IV. PROXIMITIZED MI/TI INTERFACE

The revelation of the role of MI/TI interfaces in modulation doped TI points to the significance of proximitized internal exchange coupling. Indeed, the QAH effect has been recently achieved in MI/TI/MI heterostructures.[118] As shown in Fig. 5(a), Cr-doped ZnTe, a large gap MI with favorable lattice parameters in the (111) plane matching TI, can be grown with non-magnetic TI into high quality sandwiches. The stacks possess atomically sharp interfaces and minimal Cr interfacial migration, as confirmed by energy-dispersive x-ray spectroscopy (EDS) mapping and distribution profile analysis.[118–120] Full quantization has been observed at $T$ = 30 mK [see Fig. 5(b)]. Despite the high growth temperature, the insignificant Cr diffusion across such an MI/TI interface is a salient feature, enabling reliable placement of alternating Cr-doped TI and pristine TI layers, instrumental in realizing the higher Chern number QAH state,[112] as well as spin–orbit-torque-based electrical switching of the chirality of edge current.[121]

Proximity-driven engineering offers a promising avenue for further enhancing the $T_{QAH}$ beyond the presently available sub-Kelvin regime, as well as uncovering new physics. Higher temperature QAH states may be obtained by imprinting magnetism via high-quality heterostructures with compatible MIs possessing high $T_C$ (or Néel temperature $T_N$ for antiferromagnet) while preserving the structural integrity and salient surface electronic properties of TIs. *The interface approach is a center piece at the forefront of the field.*

Recently, polarized neutron reflectometry (PNR) experiments at the EuS/$Bi_2Se_3$ interface have demonstrated that long-range magnetic order can be induced at the surface of a TI without the complication of creating spin-scattering centers in the doping case.[122] As shown in Fig. 5(c), the magnetic scattering length density (MSLD) profile reveals ferromagnetism that extends ∼2 nm into the $Bi_2Se_3$ at 5 K. The experimental spin asymmetry ratio, defined as SA = $(R^+ - R^-)/(R^+ + R^-)$, with $R^+$ or $R^-$ being the reflectivity with neutron spin parallel (+) or antiparallel (−) to the external field, provides sensitive measurement of in-plane magnetism (SA = 0 designates no magnetic moment). The temperature evolution of SA profiles in EuS film and EuS/$Bi_2Se_3$ bilayer is drastically distinct[122]—while SA becomes vanishingly small in EuS above $T_C$ ∼ 17 K, the magnetism apparently survives up to 300 K at the EuS/$Bi_2Se_3$ interface [see Fig. 5(d) for MSLD depth profiles at selected temperatures]. This enhanced magnetic behavior has been further confirmed by superconducting quantum interference device (SQUID) magnetic measurements as well as x-ray magnetic circular dichroism (XMCD) studies. It is worth emphasizing that a particularly clean, sharp and controlled *in situ* interface between EuS and TI is required in achieving the needed effective magnetic proximity coupling due to the extreme short-range nature of the exchange interaction (≲0.5 nm).[123–126] Extraordinary care is warranted in the TI growth, and the magnetic interfacial heterostructuring thereafter, to properly mitigate the adverse influence from residual chalcogen atoms since the optimal TI demands a Se/Te-rich growth condition. This intriguing discovery has opened a vibrant arena for proximitized MI/TI heterostructures.[127–138]

Extensive investigations have since been devoted to interfacial exchange coupling and the magnetic proximity effect in MI/TI systems[139] using $Y_3Fe_5O_{12}$ (YIG),[140,141] $Tm_3Fe_5O_{12}$ (TIG),[142] MnTe,[143] $Cr_2Ge_2Te_6$ (Refs. 119 and 144), and $Fe_3GeTe_2$ (Ref. 145), just to name a few. Convincing out-of-plane hysteretic AH data in platforms utilizing MIs with in-plane bulk magnetic anisotropy are not

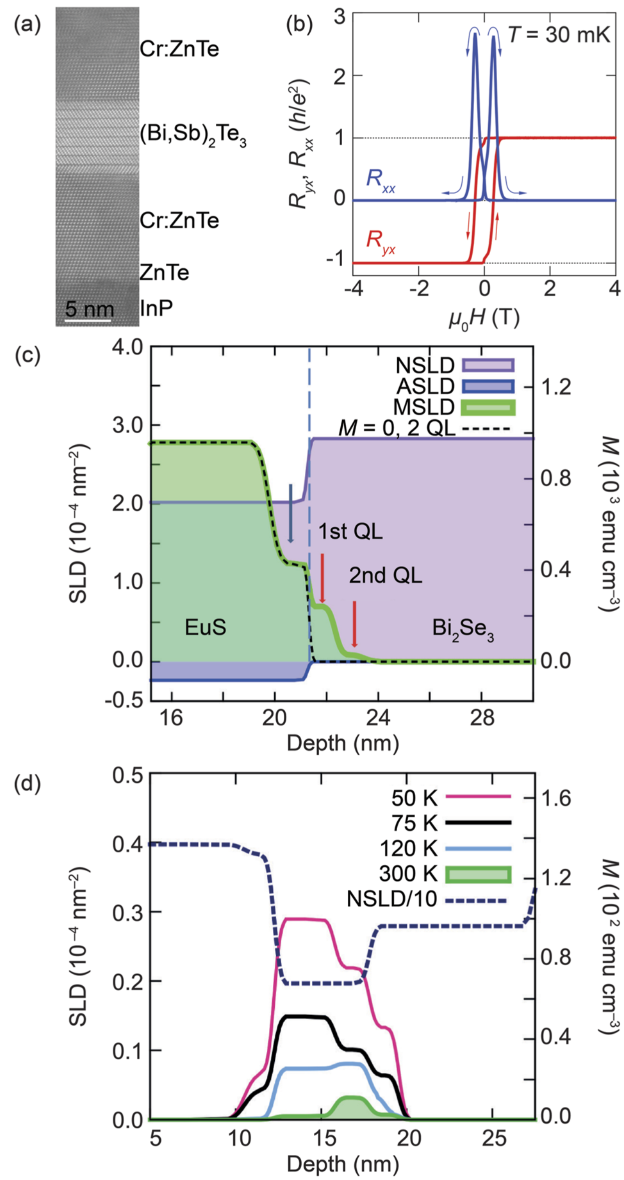


**FIG. 5.** Proximity-driven magnetic coupling at the magnetic–topological insulator interface. (a) A cross-sectional high-angle annular dark-field scanning transmission electron microscopy (HAADF-STEM) image of a Cr:ZnTe/(Bi,Sb)$_2$Te$_3$/Cr:ZnTe stack. (b) The realized QAH state at $T$ = 30 mK. (c) The PNR nuclear (NSLD), absorption (ASLD), and magnetic (MSLD) scattering length density profiles as a function of the distance from the sample surface, measured for 5 nm EuS/20 QL $Bi_2Se_3$ sample at 5 K under applied in-plane magnetic field of 1 T. The magnetization measured inside the $Bi_2Se_3$ layer is marked with red arrows, and the reduction of the in-plane component of EuS at the interface caused by a canting of the Eu magnetization vector toward the out-of-plane direction is marked with a blue arrow. The fit with zero magnetization ($M$ = 0 in 2 QL) in the $Bi_2Se_3$ layer has a large deviation from the experimental data. (d) Chemical (NSLD, dashed line) and magnetic (MSLD) depth profiles at a few selected temperatures (solid lines for 50, 75, and 120 K and green shading for 300 K). The scale on the right shows the magnetization. Adapted with permission from Watanabe *et al.*, Appl. Phys. Lett. **115**, 102403 (2019). Copyright 2019 AIP Publishing, [(a) and (b)]; Adapted with permission from Katmis *et al.*, Nature **533**, 513–516 (2016). Copyright 2016 Springer Nature Limited, [(c) and (d)].

yet available and should be pursued. Initial studies leveraging TIG, a high-$T_C$ (~560 K) MI with perpendicular magnetic anisotropy, have shown that the ordering of TI can be increased to above 400 K.[142] The $R_{yx}$ at present is admittedly small though, on the order of 0.7–2 Ω at 2 K. Inspired by the high $T_C$, it warrants future effort to improve the interfacial coupling, for instance, by growing TIG and TI *in situ* without breaking vacuum during the interface fabrication. Sandwich heterostructures taking advantages of multiple interfaces[118,119] such as TIG/TI/TIG are also desirable, should one be able to control the magnetic anisotropy of TIG as out-of-plane oriented in subsequent layers. Furthermore, proximitizing magnetic TI with antiferromagnetic (Al:)$Cr_2O_3$ enables exchange that is biased at the interface,[146,147] allowing for further tunability in QAH-based devices.[148]

## V. INTRINSIC MAGNETIC TI $MnBi_2Te_4$

Recognizing the critical importance of high-quality magnetic interfaces in QAH related physics, one may envision pushing the proximity-driven phenomena down to their ultimate limit— i.e., taking advantage of the layer-by-layer atomically ordered internal interfaces in intrinsic magnetic TIs. The promise and feasibility of such a strategy were perhaps well hinted by the large magnetic gap seen in the natural superlattice of QL $Bi_2Te_3$ and septuple layer (SL) $MnBi_2Te_4$ in Mn-doped $Bi_2Te_3$.[149] As shown in Fig. 6(a), $MnBi_2Te_4$ SLs feature intralayer ferromagnetic order and A-type interlayer antiferromagnetism. The interlayer coupling is tunable via intercalation of non-magnetic $Bi_2Te_3$ QLs, forming a family of $MnBi_2Te_4(Bi_2Te_3)_m$ with rich topological and physical properties.[150–155]

The layer sensitive magnetism in $MnBi_2Te_4$ offers a versatile platform for exploring the magnetic field driven transitions connecting the (canted) antiferromagnetic and poled ferromagnetic phases in the few SL regime, as well as the rich QAH (odd) and/or axion (even) insulator physics with precise SL number control.[156–158] As illustrated in Fig. 6(b), the QAH effect has been realized in one optimal 5 SL $MnBi_2Te_4$ (device 5 SL A), displaying $R_{yx}(0) = 0.97\ h/e^2$ and $R_{xx}(0) < 0.061\ h/e^2$ at 1.4 K.[62] While the $T_{QAH}$ for full zero-field quantization was not reported, it is likely on par with the state-of-the-art thin film results using Cr/V codoping[104] and Cr-modulation doping.[111] A comparable QAH state has also been achieved in crystal flakes with the $MnBi_2Te_4/Bi_2Te_3$ natural superlattice.[159] It has stimulated intense investigations of intrinsic magnetic TIs, although reproducing the stunning QAH result[62] in 5 SL $MnBi_2Te_4$ still appears to be challenging to date. It is likely owing to the complex interplay among crystal quality, magnetic/lattice defect, stacking/strain condition, fabrication processing, device morphology and substrate/film/capping interfaces, which leads to the often qualitatively different $R_{yx}(H)$ profiles, as shown in Fig. 6(b), e.g., for devices from a different batch (device 5 SL B)[62] or different group (device 5 SL C).[157]

As depicted in Fig. 6(c), a zero Hall plateau has been observed in 6 SL $MnBi_2Te_4$ (device 6 SL A),[160] establishing another candidate system for solid state investigation of axion physics.[161–163] The characteristic critical fields, corresponding to the small but discernible kinks in $R_{yx}$ and extrema in $R_{xx}$ for device 6 SL A,[160] are generally

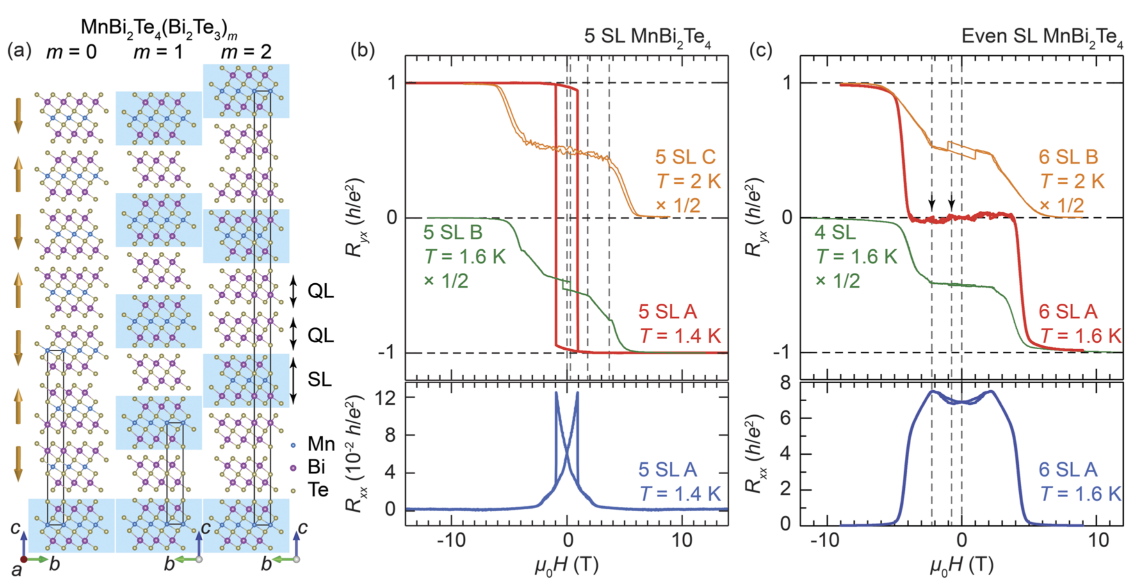


**FIG. 6.** Intrinsic magnetic insulator $MnBi_2Te_4$. (a) Crystal structure of natural superlattice of $BiMn_2Te_4(Bi_2Te_3)_m$, with $m = 0, 1, 2, \ldots$. The A-type antiferromagnetic coupling of the septuple layers (SLs) of $MnBi_2Te_4$ may be tuned by intercalating quintuple layers (QLs) of non-magnetic $Bi_2Te_3$. Field dependence of $R_{yx}$ (top) and $R_{xx}$ (bottom) for the (b) quantum anomalous Hall and (c) axion insulator like state in optimized 5 SL and 6 SL (A) $MnBi_2Te_4$, respectively. Additional 5 SL (B and C) devices and even layer samples, 6 SL (B) and 4 SL, are shown for comparison (scaled by ×1/2 and vertically shifted for clarity). Adapted with permission from Deng *et al.*, Science **367**, 895–900 (2020). Copyright 2020 American Association for the Advancement of Science, (b) 5 SL A, 5 SL B, (c) 4 SL; Adapted with permission from Liu *et al.*, Nat. Mater. **19**, 522–527 (2020). Copyright 2020 Springer Nature Limited, (c) 6 SL A; Adapted with permission from Ovchinnikov *et al.*, Nano Lett. **21**, 2544–2550 (2021). Copyright 2021 American Chemical Society, (b) 5 SL C, (c) 6 SL B.

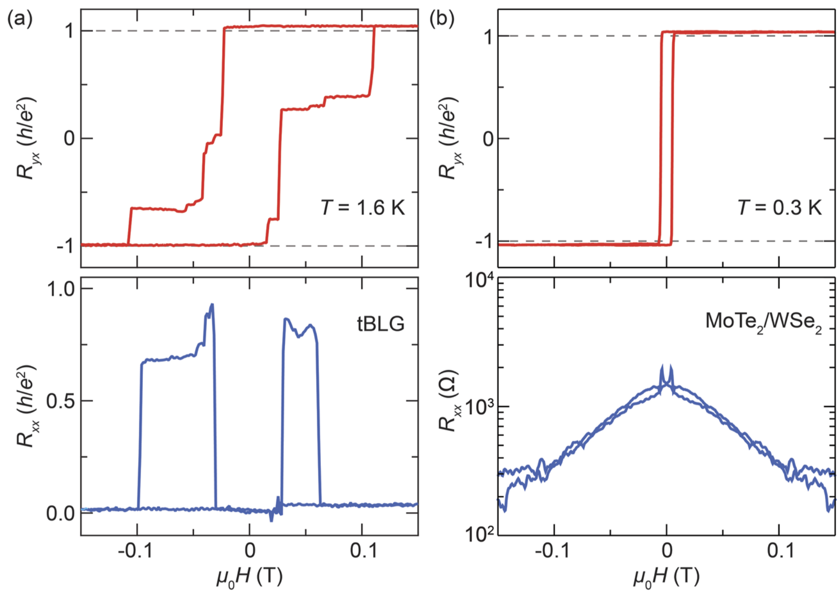


**FIG. 7.** Quantum anomalous Hall effect in Moiré materials. Field dependence of $R_{yx}$ (top) and $R_{xx}$ (bottom) for (a) magic-angle twisted bilayer graphene (tBLG) and (b) AB-stacked $MoTe_2/WSe_2$ hetero-bilayers. Adapted with permission from Serlin *et al.*, Science **367**, 900–903 (2020). Copyright 2020 American Association for the Advancement of Science, (a); Adapted with permission from Li *et al.*, Nature **600**, 641–646 (2021). Copyright 2021 Springer Nature Limited, (b).

consistent with other even SL devices (6 SL B[157] and 4 SL[62]). By means of electric field tuning, Berry-curvature-induced layer Hall (LH) effect has been uncovered in this axion insulator like regime.[164] The capability of fusing magnetism and topology at the atomic level bodes particularly well for the future advancement of topological quantum effects. To further understand the key factors underlying the magnetic and topological nature of $MnBi_2Te_4$, and QAH insulators in general, multimodal investigations are of immediate interest, synergizing magnetotransport and various scanning probes, including magnetic force microscopy (MFM),[165] microwave impedance microscopy (MIM),[166] nano-superconducting quantum interference device (nanoSQUID),[107] magneto-optical Kerr effect (MOKE) and magnetic circular dichroism (MCD).[167]

## VI. MOIRÉ MATERIALS

By interfacing 2D crystal layers, of either the same species at a small twist angle or a different kind possessing dissimilar lattice parameters, one creates artificial Moiré superlattices hosting intertwined topology and strong correlations.[168] Moiré graphene heterostructures with valley-spin-degenerate topological flat bands enable remarkable phenomena, including superconductivity,[169] correlated insulating states,[170] and when TRS is broken, orbital magnetism featuring Moiré-scale current loops.[171] Significant AH effect with strong magnetic hysteresis has been observed in twisted bilayer graphene (tBLG)[172] and ABC-trilayer graphene/hexagonal boron nitride (ABC-TLG/hBN) Moiré superlattices.[173] As shown in Fig. 7(a), a robust QAH state has been demonstrated at 1.6 K in a narrow range of density near band filling factor $\nu = 3$ in a flat-band tBLG device aligned to hBN.[63] $R_{yx}$ quantization, within 0.1% of $R_K$, has been found to survive up to 3 K, while the system displays a $T_C$ of 7.5 K.

In electrically tunable semiconductor-based hetero-bilayers, the application of an out-of-plane gating electric field modulates the bandwidth as well as the band topology by intertwining Moiré bands from different layers. At $\nu = 1$, the QAH effect was achieved at 0.3 K, upon spontaneous valley polarization in the $MoTe_2/WSe_2$ Moiré superlattice with AB configuration[64] [see Fig. 7(b)]. $R_{yx}$ remains quantized up to about 2.5 K, while staying finite up to $T_C \sim 5$–6 K. The two newly emerged Moiré platforms manifest $R_{yx} > h/e^2$ when approaching quantization, different from the TI-based phenomenology with $R_{yx} < h/e^2$, hinting that different disorder mechanisms might underpin the QAH effect owing to orbital magnetic states.

## VII. CONCLUSION AND OUTLOOK

In recent years, tremendous progress has been made in advancing topological concepts in solid state. The realization and development of the QAH effect attests to the ever-more coherent synergy between theoretical prediction/interpretation and experimental exploration/discovery of new materials. We expect the fundamental interfacial magnetism in heterostructures to fuel future development in the field. Identifying new magnetic topological systems with suitable properties for implementing the QAH effect, or exploring the interplay between magnetism and topology in general, is of paramount interest.[174–176] The versatile selective tunability of the magnetic topological interfaces further enables the investigation of the high energy physics counterparts in materials laboratory, such as dyon particles[177] and Majorana bound states,[178,179] when additional superconductivity proximity is coupled.

From an application standpoint, the QAH effect bodes particularly well for future universal quantum standard units, combining the Josephson effect in one measurement setup, where uncertainty in the 1 ppb range is a prerequisite to rival that of existing QH systems.[180] The ideally dissipation-free nature of chiral edge transport in the QAH state inspires low-energy consumption spintronics or integration to existing computing architectures as chiral interconnects.[181] Furthermore, when hybridized with superconductors, QAH insulators motivate topological quantum computing.[182] These technological breakthroughs leverage on the capability of interfacial engineering structural, chemical, magnetic, and electronic properties at the atomic scale, ideally with the robust QAH state for practical operation temperature.

Despite impressive progress using interface-inspired approaches (heterostructure or intrinsic), the $T_{\mathrm{QAH}}$ manifesting quantized $R_{yx}$ with negligible $R_{xx}$ ($\ll$1% $h/e^2$) is still limited in the sub-Kelvin regime for all $Bi_2Te_3$-derived QAH systems. It implies that mechanisms intrinsic to tetradymites, e.g., spatial inhomogeneities in thickness and/or prevailing antisite defects, might be the main culprit limiting the operation temperature, *in lieu* of the magnetic ordering, as $T_{\mathrm{C}}/T_{\mathrm{N}}$ is reasonably high of the order of tens of Kelvin. Indeed, recent analysis of non-local transport in a Corbino geometry has revealed QAH edge channels surviving up to $T_{\mathrm{C}}$ in V-doped TIs.[183] Further optimizing the bulk insulation in tetradymites,[184] or discovering an entirely new class of TIs beyond the current paradigm,[185] is beneficial toward increasing the practical relevance of the QAH effect.

In additional to MBE growth, recent development in alternative and industrial friendly routes such as sputtering[186] may bring about previously overlooked benefits, including quantum confinement and/or superior sample quality. The dynamic MBE deposition and equilibrium crystal synthesis bear dramatically different kinetics and thermodynamics. To realize the QAH state, the former route is instrumental in preparing doped films beyond the bulk solubility limit, while the latter is critical in ensuring the needed layer ordering and placement in intrinsic TIs, however not typically vice versa. Realizing intrinsic magnetic TI films capable of quantization is highly desirable, meaning material exploration. Prospects of advancing QAH physics also lie in the exploration of possibly fractional QAH by feasibly introducing the needed strong correlation, as well as the novel mechanisms exploiting, e.g., in-plane magnetization[187] and antiferromagnetism.[188] Further inspiration can also be drawn from the exciting development of twistronics, benefiting from magnetic states of orbital origin.[189]

## ACKNOWLEDGMENTS

The work was supported by the Army Research Office (Grant No. W911NF-20-2-0061), the National Science Foundation (Grant Nos. NSF-DMR 1700137 and CIQM 1231319), and the Office of Naval Research (Grant No. N00014-20-1-2306). H.C. was sponsored by the Army Research Laboratory under Cooperative Agreement No. W911NF-19-2-0015.

## AUTHOR DECLARATIONS

### Conflict of Interest

The authors have no conflicts to disclose.

### Author Contributions

**Hang Chi**: Conceptualization (equal); Writing – original draft (equal); Writing – review & editing (equal). **Jagadeesh S. Moodera**: Conceptualization (equal); Funding acquisition (equal); Project administration (equal); Supervision (equal); Writing – original draft (equal); Writing – review & editing (equal).

## DATA AVAILABILITY

The data that support the findings of this study are available from the corresponding author upon reasonable request.

## REFERENCES

[1] K. He, Y. Wang, and Q.-K. Xue, "Quantum anomalous Hall effect," Natl. Sci. Rev. **1**, 38–48 (2013).
[2] H. Weng, R. Yu, X. Hu, X. Dai, and Z. Fang, "Quantum anomalous Hall effect and related topological electronic states," Adv. Phys. **64**, 227–282 (2015).
[3] X. Kou, Y. Fan, M. Lang, P. Upadhyaya, and K. L. Wang, "Magnetic topological insulators and quantum anomalous Hall effect," Solid State Commun. **215-216**, 34–53 (2015).
[4] J. Wang, B. Lian, and S.-C. Zhang, "Quantum anomalous Hall effect in magnetic topological insulators," Phys. Scr. **T164**, 014003 (2015).
[5] C.-X. Liu, S.-C. Zhang, and X.-L. Qi, "The quantum anomalous Hall effect: Theory and experiment," Annu. Rev. Condens. Matter Phys. **7**, 301–321 (2016).
[6] C.-Z. Chang and M. Li, "Quantum anomalous Hall effect in time-reversal-symmetry breaking topological insulators," J. Phys.: Condens. Matter **28**, 123002 (2016).
[7] K. He, Y. Wang, and Q.-K. Xue, "Topological materials: Quantum anomalous Hall system," Annu. Rev. Condens. Matter Phys. **9**, 329–344 (2018).
[8] Y. Tokura, K. Yasuda, and A. Tsukazaki, "Magnetic topological insulators," Nat. Rev. Phys. **1**, 126–143 (2019).
[9] X. Kou, Y. Fan, and K. L. Wang, "Review of quantum Hall trio," J. Phys. Chem. Solids **128**, 2–23 (2019).
[10] M. Nadeem, A. R. Hamilton, M. S. Fuhrer, and X. Wang, "Quantum anomalous Hall effect in magnetic doped topological insulators and ferromagnetic spin-gapless semiconductors—A perspective review," Small **16**, 1904322 (2020).
[11] C.-Z. Chang, C.-X. Liu, and A. H. MacDonald, "Colloquium: Quantum anomalous Hall effect," arXiv:2202.13902 (2022).
[12] K. von Klitzing, T. Chakraborty, P. Kim, V. Madhavan, X. Dai, J. McIver, Y. Tokura, L. Savary, D. Smirnova, A. M. Rey, C. Felser, J. Gooth, and X. Qi, "40 years of the quantum Hall effect," Nat. Rev. Phys. **2**, 397–401 (2020).
[13] E. H. Hall, "On a new action of the magnet on electric currents," Am. J. Math. **2**, 287–292 (1879).
[14] Z. Z. Du, H.-Z. Lu, and X. C. Xie, "Nonlinear Hall effects," Nat. Rev. Phys. **3**, 744–752 (2021).
[15] E. H. Hall, "On the new action of magnetism on a permanent electric current," Am. J. Sci. **s3-20**, 161–186 (1880).
[16] N. Nagaosa, J. Sinova, S. Onoda, A. H. MacDonald, and N. P. Ong, "Anomalous Hall effect," Rev. Mod. Phys. **82**, 1539–1592 (2010).
[17] K. von Klitzing, G. Dorda, and M. Pepper, "New method for high-accuracy determination of the fine-structure constant based on quantized Hall resistance," Phys. Rev. Lett. **45**, 494–497 (1980).
[18] D. C. Tsui, H. L. Stormer, and A. C. Gossard, "Two-dimensional magnetotransport in the extreme quantum limit," Phys. Rev. Lett. **48**, 1559–1562 (1982).
[19] R. B. Laughlin, "Anomalous quantum Hall effect: An incompressible quantum fluid with fractionally charged excitations," Phys. Rev. Lett. **50**, 1395–1398 (1983).
[20] M. V. Berry, "Quantal phase factors accompanying adiabatic changes," Proc. R. Soc. London, Ser. A **392**, 45–57 (1984).
[21] D. J. Thouless, M. Kohmoto, M. P. Nightingale, and M. den Nijs, "Quantized Hall conductance in a two-dimensional periodic potential," Phys. Rev. Lett. **49**, 405–408 (1982).
[22] F. D. M. Haldane, "Model for a quantum Hall effect without Landau levels: Condensed-matter realization of the 'parity anomaly,'" Phys. Rev. Lett. **61**, 2015–2018 (1988).

[23]M. Onoda and N. Nagaosa, "Quantized anomalous Hall effect in two-dimensional ferromagnets: Quantum Hall effect in metals," Phys. Rev. Lett. **90**, 206601 (2003).
[24]R. Karplus and J. M. Luttinger, "Hall effect in ferromagnetics," Phys. Rev. **95**, 1154–1160 (1954).
[25]T. Jungwirth, Q. Niu, and A. H. MacDonald, "Anomalous Hall effect in ferromagnetic semiconductors," Phys. Rev. Lett. **88**, 207208 (2002).
[26]Z. Fang, N. Nagaosa, K. S. Takahashi, A. Asamitsu, R. Mathieu, T. Ogasawara, H. Yamada, M. Kawasaki, Y. Tokura, and K. Terakura, "The anomalous Hall effect and magnetic monopoles in momentum space," Science **302**, 92–95 (2003).
[27]F. D. M. Haldane, "Berry curvature on the fermi surface: Anomalous Hall effect as a topological fermi-liquid property," Phys. Rev. Lett. **93**, 206602 (2004).
[28]Y. Yao, L. Kleinman, A. H. MacDonald, J. Sinova, T. Jungwirth, D.-s. Wang, E. Wang, and Q. Niu, "First principles calculation of anomalous Hall conductivity in ferromagnetic bcc Fe," Phys. Rev. Lett. **92**, 037204 (2004).
[29]D. Xiao, M.-C. Chang, and Q. Niu, "Berry phase effects on electronic properties," Rev. Mod. Phys. **82**, 1959–2007 (2010).
[30]M. Z. Hasan and C. L. Kane, "Colloquium: Topological insulators," Rev. Mod. Phys. **82**, 3045–3067 (2010).
[31]X.-L. Qi and S.-C. Zhang, "Topological insulators and superconductors," Rev. Mod. Phys. **83**, 1057–1110 (2011).
[32]J. Maciejko, T. L. Hughes, and S.-C. Zhang, "The quantum spin Hall effect," Annu. Rev. Condens. Matter Phys. **2**, 31–53 (2011).
[33]C. L. Kane and E. J. Mele, "Quantum spin Hall effect in graphene," Phys. Rev. Lett. **95**, 226801 (2005).
[34]B. A. Bernevig and S.-C. Zhang, "Quantum spin Hall effect," Phys. Rev. Lett. **96**, 106802 (2006).
[35]B. A. Bernevig, T. L. Hughes, and S.-C. Zhang, "Quantum spin Hall effect and topological phase transition in HgTe quantum wells," Science **314**, 1757–1761 (2006).
[36]M. König, S. Wiedmann, C. Brüne, A. Roth, H. Buhmann, L. W. Molenkamp, X.-L. Qi, and S.-C. Zhang, "Quantum spin Hall insulator state in HgTe quantum wells," Science **318**, 766–770 (2007).
[37]A. Roth, C. Brüne, H. Buhmann, L. W. Molenkamp, J. Maciejko, X.-L. Qi, and S.-C. Zhang, "Nonlocal transport in the quantum spin Hall state," Science **325**, 294–297 (2009).
[38]C. Liu, T. L. Hughes, X.-L. Qi, K. Wang, and S.-C. Zhang, "Quantum spin Hall effect in inverted type-II semiconductors," Phys. Rev. Lett. **100**, 236601 (2008).
[39]I. Knez, R.-R. Du, and G. Sullivan, "Evidence for helical edge modes in inverted InAs/GaSb quantum wells," Phys. Rev. Lett. **107**, 136603 (2011).
[40]L. Fu, C. L. Kane, and E. J. Mele, "Topological insulators in three dimensions," Phys. Rev. Lett. **98**, 106803 (2007).
[41]H. Zhang, C.-X. Liu, X.-L. Qi, X. Dai, Z. Fang, and S.-C. Zhang, "Topological insulators in $Bi_2Se_3$, $Bi_2Te_3$, and $Sb_2Te_3$ with a single Dirac cone on the surface," Nat. Phys. **5**, 438–442 (2009).
[42]Y. Xia, D. Qian, D. Hsieh, L. Wray, A. Pal, H. Lin, A. Bansil, D. Grauer, Y. S. Hor, R. J. Cava, and M. Z. Hasan, "Observation of a large-gap topological-insulator class with a single Dirac cone on the surface," Nat. Phys. **5**, 398–402 (2009).
[43]Y. L. Chen, J. G. Analytis, J.-H. Chu, Z. K. Liu, S.-K. Mo, X. L. Qi, H. J. Zhang, D. H. Lu, X. Dai, Z. Fang, S. C. Zhang, I. R. Fisher, Z. Hussain, and Z.-X. Shen, "Experimental realization of a three-dimensional topological insulator, $Bi_2Te_3$," Science **325**, 178–181 (2009).
[44]D. Hsieh, Y. Xia, D. Qian, L. Wray, J. H. Dil, F. Meier, J. Osterwalder, L. Patthey, J. G. Checkelsky, N. P. Ong, A. V. Fedorov, H. Lin, A. Bansil, D. Grauer, Y. S. Hor, R. J. Cava, and M. Z. Hasan, "A tunable topological insulator in the spin helical Dirac transport regime," Nature **460**, 1101–1105 (2009).
[45]C.-X. Liu, X.-L. Qi, X. Dai, Z. Fang, and S.-C. Zhang, "Quantum anomalous Hall effect in $Hg_{1-y}Mn_yTe$ quantum wells," Phys. Rev. Lett. **101**, 146802 (2008).
[46]A. Budewitz, K. Bendias, P. Leubner, T. Khouri, S. Shamim, S. Wiedmann, H. Buhmann, and L. W. Molenkamp, "Quantum anomalous Hall effect in Mn doped HgTe quantum wells," arXiv:1706.05789 (2017).
[47]X.-L. Qi, T. L. Hughes, and S.-C. Zhang, "Topological field theory of time-reversal invariant insulators," Phys. Rev. B **78**, 195424 (2008).
[48]R. Yu, W. Zhang, H.-J. Zhang, S.-C. Zhang, X. Dai, and Z. Fang, "Quantized anomalous Hall effect in magnetic topological insulators," Science **329**, 61–64 (2010).
[49]K. Nomura and N. Nagaosa, "Surface-quantized anomalous Hall current and the magnetoelectric effect in magnetically disordered topological insulators," Phys. Rev. Lett. **106**, 166802 (2011).
[50]C.-Z. Chang, J. Zhang, X. Feng, J. Shen, Z. Zhang, M. Guo, K. Li, Y. Ou, P. Wei, L.-L. Wang, Z.-Q. Ji, Y. Feng, S. Ji, X. Chen, J. Jia, X. Dai, Z. Fang, S.-C. Zhang, K. He, Y. Wang, L. Lu, X.-C. Ma, and Q.-K. Xue, "Experimental observation of the quantum anomalous Hall effect in a magnetic topological insulator," Science **340**, 167–170 (2013).
[51]J. G. Checkelsky, R. Yoshimi, A. Tsukazaki, K. S. Takahashi, Y. Kozuka, J. Falson, M. Kawasaki, and Y. Tokura, "Trajectory of the anomalous Hall effect towards the quantized state in a ferromagnetic topological insulator," Nat. Phys. **10**, 731–736 (2014).
[52]X. Kou, S.-T. Guo, Y. Fan, L. Pan, M. Lang, Y. Jiang, Q. Shao, T. Nie, K. Murata, J. Tang, Y. Wang, L. He, T.-K. Lee, W.-L. Lee, and K. L. Wang, "Scale-invariant quantum anomalous Hall effect in magnetic topological insulators beyond the two-dimensional limit," Phys. Rev. Lett. **113**, 137201 (2014).
[53]A. J. Bestwick, E. J. Fox, X. Kou, L. Pan, K. L. Wang, and D. Goldhaber-Gordon, "Precise quantization of the anomalous Hall effect near zero magnetic field," Phys. Rev. Lett. **114**, 187201 (2015).
[54]A. Kandala, A. Richardella, S. Kempinger, C.-X. Liu, and N. Samarth, "Giant anisotropic magnetoresistance in a quantum anomalous Hall insulator," Nat. Commun. **6**, 7434 (2015).
[55]Y. Feng, X. Feng, Y. Ou, J. Wang, C. Liu, L. Zhang, D. Zhao, G. Jiang, S.-C. Zhang, K. He, X. Ma, Q.-K. Xue, and Y. Wang, "Observation of the zero Hall plateau in a quantum anomalous Hall insulator," Phys. Rev. Lett. **115**, 126801 (2015).
[56]C.-Z. Chang, W. Zhao, D. Y. Kim, H. Zhang, B. A. Assaf, D. Heiman, S.-C. Zhang, C. Liu, M. H. W. Chan, and J. S. Moodera, "High-precision realization of robust quantum anomalous Hall state in a hard ferromagnetic topological insulator," Nat. Mater. **14**, 473–477 (2015).
[57]K. N. Okada, Y. Takahashi, M. Mogi, R. Yoshimi, A. Tsukazaki, K. S. Takahashi, N. Ogawa, M. Kawasaki, and Y. Tokura, "Terahertz spectroscopy on Faraday and Kerr rotations in a quantum anomalous Hall state," Nat. Commun. **7**, 12245 (2016).
[58]M. Liu, W. Wang, A. R. Richardella, A. Kandala, J. Li, A. Yazdani, N. Samarth, and N. P. Ong, "Large discrete jumps observed in the transition between Chern states in a ferromagnetic topological insulator," Sci. Adv. **2**, e1600167 (2016).
[59]S. Grauer, K. M. Fijalkowski, S. Schreyeck, M. Winnerlein, K. Brunner, R. Thomale, C. Gould, and L. W. Molenkamp, "Scaling of the quantum anomalous Hall effect as an indicator of axion electrodynamics," Phys. Rev. Lett. **118**, 246801 (2017).
[60]J. Jiang, D. Xiao, F. Wang, J.-H. Shin, D. Andreoli, J. Zhang, R. Xiao, Y.-F. Zhao, M. Kayyalha, L. Zhang, K. Wang, J. Zang, C. Liu, N. Samarth, M. H. W. Chan, and C.-Z. Chang, "Concurrence of quantum anomalous Hall and topological Hall effects in magnetic topological insulator sandwich heterostructures," Nat. Mater. **19**, 732–737 (2020).
[61]S.-W. Wang, D. Xiao, Z. Dou, M. Cao, Y.-F. Zhao, N. Samarth, C.-Z. Chang, M. R. Connolly, and C. G. Smith, "Demonstration of dissipative quasihelical edge transport in quantum anomalous Hall insulators," Phys. Rev. Lett. **125**, 126801 (2020).
[62]Y. Deng, Y. Yu, M. Z. Shi, Z. Guo, Z. Xu, J. Wang, X. H. Chen, and Y. Zhang, "Quantum anomalous Hall effect in intrinsic magnetic topological insulator $MnBi_2Te_4$," Science **367**, 895–900 (2020).
[63]M. Serlin, C. L. Tschirhart, H. Polshyn, Y. Zhang, J. Zhu, K. Watanabe, T. Taniguchi, L. Balents, and A. F. Young, "Intrinsic quantized anomalous Hall effect in a moiré heterostructure," Science **367**, 900–903 (2020).
[64]T. Li, S. Jiang, B. Shen, Y. Zhang, L. Li, Z. Tao, T. Devakul, K. Watanabe, T. Taniguchi, L. Fu, J. Shan, and K. F. Mak, "Quantum anomalous Hall effect from intertwined moiré bands," Nature **600**, 641–646 (2021).
[65]H. Chi, W. Liu, and C. Uher, "Chapter 3: Growth and transport properties of tetradymite thin films," in *Materials Aspect of Thermoelectricity* (CRC Press, 2016), pp. 95–124.

[66]J. P. Heremans, R. J. Cava, and N. Samarth, "Tetradymites as thermoelectrics and topological insulators," Nat. Rev. Mater. **2**, 17049 (2017).
[67]X. Tang, Z. Li, W. Liu, Q. Zhang, and C. Uher, "A comprehensive review on $Bi_2Te_3$-based thin films: Thermoelectrics and beyond," Interdiscip. Mater. **1**, 88–115 (2022).
[68]J. Black, E. M. Conwell, L. Seigle, and C. W. Spencer, "Electrical and optical properties of some $M_2^{V\text{-}B}N_3^{VI\text{-}B}$ semiconductors," J. Phys. Chem. Solids **2**, 240–251 (1957).
[69]H. Köhler and J. Hartmann, "Burstein shift of the absorption edge of $n$-$Bi_2Se_3$," Phys. Status Solidi B **63**, 171–176 (1974).
[70]I. A. Nechaev, R. C. Hatch, M. Bianchi, D. Guan, C. Friedrich, I. Aguilera, J. L. Mi, B. B. Iversen, S. Blügel, P. Hofmann, and E. V. Chulkov, "Evidence for a direct band gap in the topological insulator $Bi_2Se_3$ from theory and experiment," Phys. Rev. B **87**, 121111 (2013).
[71]R. Sehr and L. R. Testardi, "The optical properties of $p$-type $Bi_2Te_3$–$Sb_2Te_3$ alloys between 2–15 microns," J. Phys. Chem. Solids **23**, 1219–1224 (1962).
[72]I. Lefebvre, M. Lannoo, G. Allan, A. Ibanez, J. Fourcade, J. C. Jumas, and E. Beaurepaire, "Electronic properties of antimony chalcogenides," Phys. Rev. Lett. **59**, 2471–2474 (1987).
[73]I. G. Austin, "The optical properties of bismuth telluride," Proc. Phys. Soc. **72**, 545–552 (1958).
[74]C. Y. Li, A. L. Ruoff, and C. W. Spencer, "Effect of pressure on the energy gap of $Bi_2Te_3$," J. Appl. Phys. **32**, 1733–1735 (1961).
[75]C. B. Satterthwaite and R. W. Ure, "Electrical and thermal properties of $Bi_2Te_3$," Phys. Rev. **108**, 1164–1170 (1957).
[76]H. Scherrer and S. Scherrer, "Thermoelectric properties of bismuth antimony telluride solid solutions," in *Thermoelectrics Handbook—Macro to Nano* (CRC Press, 2006), pp. 27-21–27-18.
[77]J. S. Dyck, P. Švanda, P. Lošťák, J. Horák, W. Chen, and C. Uher, "Magnetic and transport properties of the $V_2$–$VI_3$ diluted magnetic semiconductor $Sb_{2-x}Mn_xTe_3$," J. Appl. Phys. **94**, 7631–7635 (2003).
[78]Y. S. Hor, P. Roushan, H. Beidenkopf, J. Seo, D. Qu, J. G. Checkelsky, L. A. Wray, D. Hsieh, Y. Xia, S.-Y. Xu, D. Qian, M. Z. Hasan, N. P. Ong, A. Yazdani, and R. J. Cava, "Development of ferromagnetism in the doped topological insulator $Bi_{2-x}Mn_xTe_3$," Phys. Rev. B **81**, 195203 (2010).
[79]H. Chi, G. Tan, M. G. Kanatzidis, Q. Li, and C. Uher, "A low-temperature study of manganese-induced ferromagnetism and valence band convergence in tin telluride," Appl. Phys. Lett. **108**, 182101 (2016).
[80]J. S. Dyck, P. Hajek, P. Lostak, and C. Uher, "Diluted magnetic semiconductors based on $Sb_{2-x}V_xTe_3$ ($0.01 \le x \le 0.03$)," Phys. Rev. B **65**, 115212 (2002).
[81]J. S. Dyck, Č. Drašar, P. Lošťák, and C. Uher, "Low-temperature ferromagnetic properties of the diluted magnetic semiconductor $Sb_{2-x}Cr_xTe_3$," Phys. Rev. B **71**, 115214 (2005).
[82]Z. Zhou, Y.-J. Chien, and C. Uher, "Thin-film ferromagnetic semiconductors based on $Sb_{2-x}V_xTe_3$ with $T_C$ of 177 K," Appl. Phys. Lett. **87**, 112503 (2005).
[83]Z. Zhou, Y.-J. Chien, and C. Uher, "Thin film dilute ferromagnetic semiconductors $Sb_{2-x}Cr_xTe_3$ with a Curie temperature up to 190 K," Phys. Rev. B **74**, 224418 (2006).
[84]F. J. Himpsel, J. E. Ortega, G. J. Mankey, and R. F. Willis, "Magnetic nanostructures," Adv. Phys. **47**, 511–597 (1998).
[85]L. Zhang, T. Helm, H. Lin, F. Fan, C. Le, Y. Sun, A. Markou, and C. Felser, "Quantum oscillations in ferromagnetic (Sb, V)$_2$Te$_3$ topological insulator thin films," Adv. Mater. **33**, 2102107 (2021).
[86]P. P. J. Haazen, J.-B. Laloë, T. J. Nummy, H. J. M. Swagten, P. Jarillo-Herrero, D. Heiman, and J. S. Moodera, "Ferromagnetism in thin-film Cr-doped topological insulator $Bi_2Se_3$," Appl. Phys. Lett. **100**, 082404 (2012).
[87]J. A. Krieger, C.-Z. Chang, M.-A. Husanu, D. Sostina, A. Ernst, M. M. Otrokov, T. Prokscha, T. Schmitt, A. Suter, M. G. Vergniory, E. V. Chulkov, J. S. Moodera, V. N. Strocov, and Z. Salman, "Spectroscopic perspective on the interplay between electronic and magnetic properties of magnetically doped topological insulators," Phys. Rev. B **96**, 184402 (2017).
[88]M. Büttiker, "Four-terminal phase-coherent conductance," Phys. Rev. Lett. **57**, 1761–1764 (1986).
[89]M. Büttiker, "Absence of backscattering in the quantum Hall effect in multiprobe conductors," Phys. Rev. B **38**, 9375–9389 (1988).
[90]C.-Z. Chang, W. Zhao, D. Y. Kim, P. Wei, J. K. Jain, C. Liu, M. H. W. Chan, and J. S. Moodera, "Zero-field dissipationless chiral edge transport and the nature of dissipation in the quantum anomalous Hall state," Phys. Rev. Lett. **115**, 057206 (2015).
[91]K. Yasuda, M. Mogi, R. Yoshimi, A. Tsukazaki, K. S. Takahashi, M. Kawasaki, F. Kagawa, and Y. Tokura, "Quantized chiral edge conduction on domain walls of a magnetic topological insulator," Science **358**, 1311–1314 (2017).
[92]I. T. Rosen, E. J. Fox, X. Kou, L. Pan, K. L. Wang, and D. Goldhaber-Gordon, "Chiral transport along magnetic domain walls in the quantum anomalous Hall effect," npj Quantum Mater. **2**, 69 (2017).
[93]X. Kou, L. Pan, J. Wang, Y. Fan, E. S. Choi, W.-L. Lee, T. Nie, K. Murata, Q. Shao, S.-C. Zhang, and K. L. Wang, "Metal-to-insulator switching in quantum anomalous Hall states," Nat. Commun. **6**, 8474 (2015).
[94]C.-Z. Chang, W. Zhao, J. Li, J. K. Jain, C. Liu, J. S. Moodera, and M. H. W. Chan, "Observation of the quantum anomalous Hall insulator to Anderson insulator quantum phase transition and its scaling behavior," Phys. Rev. Lett. **117**, 126802 (2016).
[95]M. Kawamura, M. Mogi, R. Yoshimi, A. Tsukazaki, Y. Kozuka, K. S. Takahashi, M. Kawasaki, and Y. Tokura, "Topological quantum phase transition in magnetic topological insulator upon magnetization rotation," Phys. Rev. B **98**, 140404 (2018).
[96]C. Liu, Y. Ou, Y. Feng, G. Jiang, W. Wu, S. Li, Z. Cheng, K. He, X. Ma, Q. Xue, and Y. Wang, "Distinct quantum anomalous Hall ground states induced by magnetic disorders," Phys. Rev. X **10**, 041063 (2020).
[97]X. Wu, D. Xiao, C.-Z. Chen, J. Sun, L. Zhang, M. H. W. Chan, N. Samarth, X. C. Xie, X. Lin, and C.-Z. Chang, "Scaling behavior of the quantum phase transition from a quantum-anomalous-Hall insulator to an axion insulator," Nat. Commun. **11**, 4532 (2020).
[98]M. Götz, K. M. Fijalkowski, E. Pesel, M. Hartl, S. Schreyeck, M. Winnerlein, S. Grauer, H. Scherer, K. Brunner, C. Gould, F. J. Ahlers, and L. W. Molenkamp, "Precision measurement of the quantized anomalous Hall resistance at zero magnetic field," Appl. Phys. Lett. **112**, 072102 (2018).
[99]E. J. Fox, I. T. Rosen, Y. Yang, G. R. Jones, R. E. Elmquist, X. Kou, L. Pan, K. L. Wang, and D. Goldhaber-Gordon, "Part-per-million quantization and current-induced breakdown of the quantum anomalous Hall effect," Phys. Rev. B **98**, 075145 (2018).
[100]Y. Okazaki, T. Oe, M. Kawamura, R. Yoshimi, S. Nakamura, S. Takada, M. Mogi, K. S. Takahashi, A. Tsukazaki, M. Kawasaki, Y. Tokura, and N.-H. Kaneko, "Precise resistance measurement of quantum anomalous Hall effect in magnetic heterostructure film of topological insulator," Appl. Phys. Lett. **116**, 143101 (2020).
[101]Y. Okazaki, T. Oe, M. Kawamura, R. Yoshimi, S. Nakamura, S. Takada, M. Mogi, K. S. Takahashi, A. Tsukazaki, M. Kawasaki, Y. Tokura, and N.-H. Kaneko, "Quantum anomalous Hall effect with a permanent magnet defines a quantum resistance standard," Nat. Phys. **18**, 25–29 (2022).
[102]M. Kawamura, R. Yoshimi, A. Tsukazaki, K. S. Takahashi, M. Kawasaki, and Y. Tokura, "Current-driven instability of the quantum anomalous Hall effect in ferromagnetic topological insulators," Phys. Rev. Lett. **119**, 016803 (2017).
[103]G. Lippertz, A. Bliesener, A. Uday, L. M. C. Pereira, A. A. Taskin, and Y. Ando, "Current-induced breakdown of the quantum anomalous Hall effect," Phys. Rev. B **106**, 045419 (2022).
[104]Y. Ou, C. Liu, G. Jiang, Y. Feng, D. Zhao, W. Wu, X. X. Wang, W. Li, C. Song, L. L. Wang, W. Wang, W. Wu, Y. Wang, K. He, X. C. Ma, and Q. K. Xue, "Enhancing the quantum anomalous Hall effect by magnetic codoping in a topological insulator," Adv. Mater. **30**, 1703062 (2018).
[105]S. Grauer, S. Schreyeck, M. Winnerlein, K. Brunner, C. Gould, and L. W. Molenkamp, "Coincidence of superparamagnetism and perfect quantization in the quantum anomalous Hall state," Phys. Rev. B **92**, 201304 (2015).
[106]I. Lee, C. K. Kim, J. Lee, S. J. L. Billinge, R. Zhong, J. A. Schneeloch, T. Liu, T. Valla, J. M. Tranquada, G. Gu, and J. C. S. Davis, "Imaging Dirac-mass disorder from magnetic dopant atoms in the ferromagnetic topological insulator $Cr_x(Bi_{0.1}Sb_{0.9})_{2-x}Te_3$," Proc. Natl. Acad. Sci. U. S. A. **112**, 1316–1321 (2015).
[107]E. O. Lachman, A. F. Young, A. Richardella, J. Cuppens, H. R. Naren, Y. Anahory, A. Y. Meltzer, A. Kandala, S. Kempinger, Y. Myasoedov, M. E. Huber, N. Samarth, and E. Zeldov, "Visualization of superparamagnetic dynamics in magnetic topological insulators," Sci. Adv. **1**, e1500740 (2015).

[108] X. Feng, Y. Feng, J. Wang, Y. Ou, Z. Hao, C. Liu, Z. Zhang, L. Zhang, C. Lin, J. Liao, Y. Li, L. L. Wang, S. H. Ji, X. Chen, X. Ma, S. C. Zhang, Y. Wang, K. He, and Q. K. Xue, "Thickness dependence of the quantum anomalous Hall effect in magnetic topological insulator films," Adv. Mater. **28**, 6386–6390 (2016).

[109] Y. Ji, Z. Liu, P. Zhang, L. Li, S. Qi, P. Chen, Y. Zhang, Q. Yao, Z. Liu, K. L. Wang, Z. Qiao, and X. Kou, "Thickness-driven quantum anomalous Hall phase transition in magnetic topological insulator thin films," ACS Nano **16**, 1134–1141 (2022).

[110] H. Chi, W. Liu, K. Sun, X. Su, G. Wang, P. Lošt'ák, V. Kucek, Č. Drašar, and C. Uher, "Low-temperature transport properties of Tl-doped $Bi_2Te_3$ single crystals," Phys. Rev. B **88**, 045202 (2013).

[111] M. Mogi, R. Yoshimi, A. Tsukazaki, K. Yasuda, Y. Kozuka, K. S. Takahashi, M. Kawasaki, and Y. Tokura, "Magnetic modulation doping in topological insulators toward higher-temperature quantum anomalous Hall effect," Appl. Phys. Lett. **107**, 182401 (2015).

[112] Y.-F. Zhao, R. Zhang, R. Mei, L.-J. Zhou, H. Yi, Y.-Q. Zhang, J. Yu, R. Xiao, K. Wang, N. Samarth, M. H. W. Chan, C.-X. Liu, and C.-Z. Chang, "Tuning the Chern number in quantum anomalous Hall insulators," Nature **588**, 419–423 (2020).

[113] G. Jiang, Y. Feng, W. Wu, S. Li, Y. Bai, Y. Li, Q. Zhang, L. Gu, X. Feng, D. Zhang, C. Song, L. Wang, W. Li, X.-C. Ma, Q.-K. Xue, Y. Wang, and K. He, "Quantum anomalous Hall multilayers grown by molecular beam epitaxy," Chin. Phys. Lett. **35**, 076802 (2018).

[114] H. Jiang, Z. Qiao, H. Liu, and Q. Niu, "Quantum anomalous Hall effect with tunable Chern number in magnetic topological insulator film," Phys. Rev. B **85**, 045445 (2012).

[115] J. Wang, B. Lian, H. Zhang, Y. Xu, and S.-C. Zhang, "Quantum anomalous Hall effect with higher plateaus," Phys. Rev. Lett. **111**, 136801 (2013).

[116] Y.-F. Zhao, R. Zhang, L.-J. Zhou, R. Mei, Z.-J. Yan, M. H. W. Chan, C.-X. Liu, and C.-Z. Chang, "Zero magnetic field plateau phase transition in higher Chern number quantum anomalous Hall insulators," Phys. Rev. Lett. **128**, 216801 (2022).

[117] M. Mogi, Y. Okamura, M. Kawamura, R. Yoshimi, K. Yasuda, A. Tsukazaki, K. S. Takahashi, T. Morimoto, N. Nagaosa, M. Kawasaki, Y. Takahashi, and Y. Tokura, "Experimental signature of the parity anomaly in a semi-magnetic topological insulator," Nat. Phys. **18**, 390–394 (2022).

[118] R. Watanabe, R. Yoshimi, M. Kawamura, M. Mogi, A. Tsukazaki, X. Z. Yu, K. Nakajima, K. S. Takahashi, M. Kawasaki, and Y. Tokura, "Quantum anomalous Hall effect driven by magnetic proximity coupling in all-telluride based heterostructure," Appl. Phys. Lett. **115**, 102403 (2019).

[119] M. Mogi, T. Nakajima, V. Ukleev, A. Tsukazaki, R. Yoshimi, M. Kawamura, K. S. Takahashi, T. Hanashima, K. Kakurai, T.-h. Arima, M. Kawasaki, and Y. Tokura, "Large anomalous Hall effect in topological insulators with proximitized ferromagnetic insulators," Phys. Rev. Lett. **123**, 016804 (2019).

[120] M. Mogi, M. Kawamura, A. Tsukazaki, R. Yoshimi, K. S. Takahashi, M. Kawasaki, and Y. Tokura, "Tailoring tricolor structure of magnetic topological insulator for robust axion insulator," Sci. Adv. **3**, eaao1669 (2017).

[121] W. Yuan, L.-J. Zhou, K. Yang, Y.-F. Zhao, R. Zhang, Z. Yan, D. Zhuo, R. Mei, M. H. W. Chan, M. Kayyalha, C.-X. Liu, and C.-Z. Chang, "Electrical switching of the edge current chirality in quantum anomalous Hall insulators," arXiv:2205.01581 (2022).

[122] F. Katmis, V. Lauter, F. S. Nogueira, B. A. Assaf, M. E. Jamer, P. Wei, B. Satpati, J. W. Freeland, I. Eremin, D. Heiman, P. Jarillo-Herrero, and J. S. Moodera, "A high-temperature ferromagnetic topological insulating phase by proximity coupling," Nature **533**, 513–516 (2016).

[123] J. M. D. Coey, "5.2: Exchange interactions," in *Magnetism and Magnetic Materials* (Cambridge University Press, 2010), p. 135.

[124] G.-X. Miao, M. Münzenberg, and J. S. Moodera, "Tunneling path toward spintronics," Rep. Prog. Phys. **74**, 036501 (2011).

[125] B. Li, N. Roschewsky, B. A. Assaf, M. Eich, M. Epstein-Martin, D. Heiman, M. Münzenberg, and J. S. Moodera, "Superconducting spin switch with infinite magnetoresistance induced by an internal exchange field," Phys. Rev. Lett. **110**, 097001 (2013).

[126] G.-X. Miao and J. S. Moodera, "Spin manipulation with magnetic semiconductor barriers," Phys. Chem. Chem. Phys. **17**, 751–761 (2015).

[127] P. Wei, F. Katmis, B. A. Assaf, H. Steinberg, P. Jarillo-Herrero, D. Heiman, and J. S. Moodera, "Exchange-coupling-induced symmetry breaking in topological insulators," Phys. Rev. Lett. **110**, 186807 (2013).

[128] M. Li, C.-Z. Chang, B. J. Kirby, M. E. Jamer, W. Cui, L. Wu, P. Wei, Y. Zhu, D. Heiman, J. Li, and J. S. Moodera, "Proximity-driven enhanced magnetic order at ferromagnetic-insulator–magnetic-topological-insulator interface," Phys. Rev. Lett. **115**, 087201 (2015).

[129] C. Lee, F. Katmis, P. Jarillo-Herrero, J. S. Moodera, and N. Gedik, "Direct measurement of proximity-induced magnetism at the interface between a topological insulator and a ferromagnet," Nat. Commun. **7**, 12014 (2016).

[130] J. Kim, K.-W. Kim, H. Wang, J. Sinova, and R. Wu, "Understanding the giant enhancement of exchange interaction in $Bi_2Se_3$-EuS heterostructures," Phys. Rev. Lett. **119**, 027201 (2017).

[131] M. Li, Q. Song, W. Zhao, J. A. Garlow, T.-H. Liu, L. Wu, Y. Zhu, J. S. Moodera, M. H. W. Chan, G. Chen, and C.-Z. Chang, "Dirac-electron-mediated magnetic proximity effect in topological insulator/magnetic insulator heterostructures," Phys. Rev. B **96**, 201301(R) (2017).

[132] Q. I. Yang and A. Kapitulnik, "Two-stage proximity-induced gap opening in topological-insulator–insulating-ferromagnet $(Bi_xSb_{1-x})_2Te_3$–EuS bilayers," Phys. Rev. B **98**, 081403 (2018).

[133] D. Rakhmilevich, F. Wang, W. Zhao, M. H. W. Chan, J. S. Moodera, C. Liu, and C.-Z. Chang, "Unconventional planar Hall effect in exchange-coupled topological insulator–ferromagnetic insulator heterostructures," Phys. Rev. B **98**, 094404 (2018).

[134] J. A. Krieger, Y. Ou, M. Caputo, A. Chikina, M. Döbeli, M.-A. Husanu, I. Keren, T. Prokscha, A. Suter, C.-Z. Chang, J. S. Moodera, V. N. Strocov, and Z. Salman, "Do topology and ferromagnetism cooperate at the EuS/$Bi_2Se_3$ interface?," Phys. Rev. B **99**, 064423 (2019).

[135] S. Mathimalar, S. Sasmal, A. Bhardwaj, S. Abhaya, R. Pothala, S. Chaudhary, B. Satpati, and K. V. Raman, "Signature of gate-controlled magnetism and localization effects at $Bi_2Se_3$/EuS interface," npj Quantum Mater. **5**, 64 (2020).

[136] A. I. Figueroa, F. Bonell, M. G. Cuxart, M. Valvidares, P. Gargiani, G. van der Laan, A. Mugarza, and S. O. Valenzuela, "Absence of magnetic proximity effect at the interface of $Bi_2Se_3$ and $(Bi,Sb)_2Te_3$ with EuS," Phys. Rev. Lett. **125**, 226801 (2020).

[137] H. L. Meyerheim, A. Ernst, K. Mohseni, A. Polyakov, I. V. Maznichenko, P. A. Buczek, A. Coati, and S. S. P. Parkin, "Structure and magnetism of EuS on $Bi_2Se_3$(0001)," Phys. Status Solidi B **258**, 2000290 (2021).

[138] N. Andrejevic, Z. Chen, T. Nguyen, L. Fan, H. Heiberger, L.-J. Zhou, Y.-F. Zhao, C.-Z. Chang, A. Grutter, and M. Li, "Elucidating proximity magnetism through polarized neutron reflectometry and machine learning," Appl. Phys. Rev. **9**, 011421 (2022).

[139] S. Bhattacharyya, G. Akhgar, M. Gebert, J. Karel, M. T. Edmonds, and M. S. Fuhrer, "Recent progress in proximity coupling of magnetism to topological insulators," Adv. Mater. **33**, 2007795 (2021).

[140] Z. Jiang, C.-Z. Chang, C. Tang, P. Wei, J. S. Moodera, and J. Shi, "Independent tuning of electronic properties and induced ferromagnetism in topological insulators with heterostructure approach," Nano Lett. **15**, 5835–5840 (2015).

[141] C. Tang, Q. Song, C.-Z. Chang, Y. Xu, Y. Ohnuma, M. Matsuo, Y. Liu, W. Yuan, Y. Yao, J. S. Moodera, S. Maekawa, W. Han, and J. Shi, "Dirac surface state-modulated spin dynamics in a ferrimagnetic insulator at room temperature," Sci. Adv. **4**, eaas8660 (2018).

[142] C. Tang, C.-Z. Chang, G. Zhao, Y. Liu, Z. Jiang, C.-X. Liu, M. R. McCartney, D. J. Smith, T. Chen, J. S. Moodera, and J. Shi, "Above 400-K robust perpendicular ferromagnetic phase in a topological insulator," Sci. Adv. **3**, e1700307 (2017).

[143] Q. L. He, G. Yin, A. J. Grutter, L. Pan, X. Che, G. Yu, D. A. Gilbert, S. M. Disseler, Y. Liu, P. Shafer, B. Zhang, Y. Wu, B. J. Kirby, E. Arenholz, R. K. Lake, X. Han, and K. L. Wang, "Exchange-biasing topological charges by antiferromagnetism," Nat. Commun. **9**, 2767 (2018).

[144] M. Mogi, K. Yasuda, R. Fujimura, R. Yoshimi, N. Ogawa, A. Tsukazaki, M. Kawamura, K. S. Takahashi, M. Kawasaki, and Y. Tokura, "Current-induced switching of proximity-induced ferromagnetic surface states in a topological insulator," Nat. Commun. **12**, 1404 (2021).

[145] H. Wang, Y. Liu, P. Wu, W. Hou, Y. Jiang, X. Li, C. Pandey, D. Chen, Q. Yang, H. Wang, D. Wei, N. Lei, W. Kang, L. Wen, T. Nie, W. Zhao, and

K. L. Wang, "Above room-temperature ferromagnetism in wafer-scale two-dimensional van der Waals $Fe_3GeTe_2$ tailored by a topological insulator," ACS Nano **14**, 10045–10053 (2020).
[146] L. Pan, A. Grutter, P. Zhang, X. Che, T. Nozaki, A. Stern, M. Street, B. Zhang, B. Casas, Q. L. He, E. S. Choi, S. M. Disseler, D. A. Gilbert, G. Yin, Q. Shao, P. Deng, Y. Wu, X. Liu, X. Kou, S. Masashi, X. Han, C. Binek, S. Chambers, J. Xia, and K. L. Wang, "Observation of quantum anomalous Hall effect and exchange interaction in topological insulator/antiferromagnet heterostructure," Adv. Mater. **32**, 2001460 (2020).
[147] P. Zhang, P. P. Balakrishnan, C. Eckberg, P. Deng, T. Nozaki, S. Chong, P. Quarterman, M. E. Holtz, B. B. Maranville, L. Pan, E. Emmanouilidou, N. Ni, M. Sahashi, A. Grutter, and K. L. Wang, "Exchange-biased quantum anomalous Hall effect," arXiv:2205.03596 (2022).
[148] H. Fu, C.-X. Liu, and B. Yan, "Exchange bias and quantum anomalous Hall effect in the $MnBi_2Te_4/CrI_3$ heterostructure," Sci. Adv. **6**, eaaz0948 (2020).
[149] E. D. L. Rienks, S. Wimmer, J. Sánchez-Barriga, O. Caha, P. S. Mandal, J. Růžička, A. Ney, H. Steiner, V. V. Volobuev, H. Groiss, M. Albu, G. Kothleitner, J. Michalička, S. A. Khan, J. Minár, H. Ebert, G. Bauer, F. Freyse, A. Varykhalov, O. Rader, and G. Springholz, "Large magnetic gap at the Dirac point in $Bi_2Te_3/MnBi_2Te_4$ heterostructures," Nature **576**, 423–428 (2019).
[150] J. Li, Y. Li, S. Du, Z. Wang, B.-L. Gu, S.-C. Zhang, K. He, W. Duan, and Y. Xu, "Intrinsic magnetic topological insulators in van der Waals layered $MnBi_2Te_4$-family materials," Sci. Adv. **5**, eaaw5685 (2019).
[151] Y. Gong, J. Guo, J. Li, K. Zhu, M. Liao, X. Liu, Q. Zhang, L. Gu, L. Tang, X. Feng, D. Zhang, W. Li, C. Song, L. Wang, P. Yu, X. Chen, Y. Wang, H. Yao, W. Duan, Y. Xu, S.-C. Zhang, X. Ma, Q.-K. Xue, and K. He, "Experimental realization of an intrinsic magnetic topological insulator," Chin. Phys. Lett. **36**, 076801 (2019).
[152] M. M. Otrokov, I. I. Klimovskikh, H. Bentmann, D. Estyunin, A. Zeugner, Z. S. Aliev, S. Gaß, A. U. B. Wolter, A. V. Koroleva, A. M. Shikin, M. Blanco-Rey, M. Hoffmann, I. P. Rusinov, A. Y. Vyazovskaya, S. V. Eremeev, Y. M. Koroteev, V. M. Kuznetsov, F. Freyse, J. Sánchez-Barriga, I. R. Amiraslanov, M. B. Babanly, N. T. Mamedov, N. A. Abdullayev, V. N. Zverev, A. Alfonsov, V. Kataev, B. Büchner, E. F. Schwier, S. Kumar, A. Kimura, L. Petaccia, G. Di Santo, R. C. Vidal, S. Schatz, K. Kißner, M. Ünzelmann, C. H. Min, S. Moser, T. R. F. Peixoto, F. Reinert, A. Ernst, P. M. Echenique, A. Isaeva, and E. V. Chulkov, "Prediction and observation of an antiferromagnetic topological insulator," Nature **576**, 416–422 (2019).
[153] J. Wu, F. Liu, C. Liu, Y. Wang, C. Li, Y. Lu, S. Matsuishi, and H. Hosono, "Toward 2D magnets in the $(MnBi_2Te_4)(Bi_2Te_3)_n$ bulk crystal," Adv. Mater. **32**, 2001815 (2020).
[154] W. Ning and Z. Mao, "Recent advancements in the study of intrinsic magnetic topological insulators and magnetic Weyl semimetals," APL Mater. **8**, 090701 (2020).
[155] Y. Zhao and Q. Liu, "Routes to realize the axion-insulator phase in $MnBi_2Te_4(Bi_2Te_3)_n$ family," Appl. Phys. Lett. **119**, 060502 (2021).
[156] S. Yang, X. Xu, Y. Zhu, R. Niu, C. Xu, Y. Peng, X. Cheng, X. Jia, Y. Huang, X. Xu, J. Lu, and Y. Ye, "Odd-even layer-number effect and layer-dependent magnetic phase diagrams in $MnBi_2Te_4$," Phys. Rev. X **11**, 011003 (2021).
[157] D. Ovchinnikov, X. Huang, Z. Lin, Z. Fei, J. Cai, T. Song, M. He, Q. Jiang, C. Wang, H. Li, Y. Wang, Y. Wu, D. Xiao, J.-H. Chu, J. Yan, C.-Z. Chang, Y.-T. Cui, and X. Xu, "Intertwined topological and magnetic orders in atomically thin chern insulator $MnBi_2Te_4$," Nano Lett. **21**, 2544–2550 (2021).
[158] Y.-F. Zhao, L.-J. Zhou, F. Wang, G. Wang, T. Song, D. Ovchinnikov, H. Yi, R. Mei, K. Wang, M. H. W. Chan, C.-X. Liu, X. Xu, and C.-Z. Chang, "Even–odd layer-dependent anomalous Hall effect in topological magnet $MnBi_2Te_4$ thin films," Nano Lett. **21**, 7691–7698 (2021).
[159] H. Deng, Z. Chen, A. Wołoś, M. Konczykowski, K. Sobczak, J. Sitnicka, I. V. Fedorchenko, J. Borysiuk, T. Heider, Ł. Pluciński, K. Park, A. B. Georgescu, J. Cano, and L. Krusin-Elbaum, "High-temperature quantum anomalous Hall regime in a $MnBi_2Te_4/Bi_2Te_3$ superlattice," Nat. Phys. **17**, 36–42 (2021).
[160] C. Liu, Y. Wang, H. Li, Y. Wu, Y. Li, J. Li, K. He, Y. Xu, J. Zhang, and Y. Wang, "Robust axion insulator and Chern insulator phases in a two-dimensional antiferromagnetic topological insulator," Nat. Mater. **19**, 522–527 (2020).
[161] M. Mogi, M. Kawamura, R. Yoshimi, A. Tsukazaki, Y. Kozuka, N. Shirakawa, K. S. Takahashi, M. Kawasaki, and Y. Tokura, "A magnetic heterostructure of topological insulators as a candidate for an axion insulator," Nat. Mater. **16**, 516–521 (2017).
[162] D. Xiao, J. Jiang, J.-H. Shin, W. Wang, F. Wang, Y.-F. Zhao, C. Liu, W. Wu, M. H. W. Chan, N. Samarth, and C.-Z. Chang, "Realization of the axion insulator state in quantum anomalous Hall sandwich heterostructures," Phys. Rev. Lett. **120**, 056801 (2018).
[163] K. M. Fijalkowski, N. Liu, M. Hartl, M. Winnerlein, P. Mandal, A. Coschizza, A. Fothergill, S. Grauer, S. Schreyeck, K. Brunner, M. Greiter, R. Thomale, C. Gould, and L. W. Molenkamp, "Any axion insulator must be a bulk three-dimensional topological insulator," Phys. Rev. B **103**, 235111 (2021).
[164] A. Gao, Y.-F. Liu, C. Hu, J.-X. Qiu, C. Tzschaschel, B. Ghosh, S.-C. Ho, D. Bérubé, R. Chen, H. Sun, Z. Zhang, X.-Y. Zhang, Y.-X. Wang, N. Wang, Z. Huang, C. Felser, A. Agarwal, T. Ding, H.-J. Tien, A. Akey, J. Gardener, B. Singh, K. Watanabe, T. Taniguchi, K. S. Burch, D. C. Bell, B. B. Zhou, W. Gao, H.-Z. Lu, A. Bansil, H. Lin, T.-R. Chang, L. Fu, Q. Ma, N. Ni, and S.-Y. Xu, "Layer Hall effect in a 2D topological axion antiferromagnet," Nature **595**, 521–525 (2021).
[165] W. Wang, Y. Ou, C. Liu, Y. Wang, K. He, Q.-K. Xue, and W. Wu, "Direct evidence of ferromagnetism in a quantum anomalous Hall system," Nat. Phys. **14**, 791–795 (2018).
[166] M. Allen, Y. Cui, E. Y. Ma, M. Mogi, M. Kawamura, I. C. Fulga, D. Goldhaber-Gordon, Y. Tokura, and Z.-X. Shen, "Visualization of an axion insulating state at the transition between 2 chiral quantum anomalous Hall states," Proc. Natl. Acad. Sci. U. S. A. **116**, 14511–14515 (2019).
[167] K. F. Mak, J. Shan, and D. C. Ralph, "Probing and controlling magnetic states in 2D layered magnetic materials," Nat. Rev. Phys. **1**, 646–661 (2019).
[168] E. Y. Andrei, D. K. Efetov, P. Jarillo-Herrero, A. H. MacDonald, K. F. Mak, T. Senthil, E. Tutuc, A. Yazdani, and A. F. Young, "The marvels of moiré materials," Nat. Rev. Mater. **6**, 201–206 (2021).
[169] Y. Cao, V. Fatemi, S. Fang, K. Watanabe, T. Taniguchi, E. Kaxiras, and P. Jarillo-Herrero, "Unconventional superconductivity in magic-angle graphene superlattices," Nature **556**, 43–50 (2018).
[170] Y. Cao, V. Fatemi, A. Demir, S. Fang, S. L. Tomarken, J. Y. Luo, J. D. Sanchez-Yamagishi, K. Watanabe, T. Taniguchi, E. Kaxiras, R. C. Ashoori, and P. Jarillo-Herrero, "Correlated insulator behaviour at half-filling in magic-angle graphene superlattices," Nature **556**, 80–84 (2018).
[171] J. Liu and X. Dai, "Orbital magnetic states in moiré graphene systems," Nat. Rev. Phys. **3**, 367–382 (2021).
[172] A. L. Sharpe, E. J. Fox, A. W. Barnard, J. Finney, K. Watanabe, T. Taniguchi, M. A. Kastner, and D. Goldhaber-Gordon, "Emergent ferromagnetism near three-quarters filling in twisted bilayer graphene," Science **365**, 605–608 (2019).
[173] G. Chen, A. L. Sharpe, E. J. Fox, Y.-H. Zhang, S. Wang, L. Jiang, B. Lyu, H. Li, K. Watanabe, T. Taniguchi, Z. Shi, T. Senthil, D. Goldhaber-Gordon, Y. Zhang, and F. Wang, "Tunable correlated Chern insulator and ferromagnetism in a moiré superlattice," Nature **579**, 56–61 (2020).
[174] S. Nakatsuji and R. Arita, "Topological magnets: Functions based on Berry phase and multipoles," Annu. Rev. Condens. Matter Phys. **13**, 119–142 (2022).
[175] Q. L. He, T. L. Hughes, N. P. Armitage, Y. Tokura, and K. L. Wang, "Topological spintronics and magnetoelectronics," Nat. Mater. **21**, 15–23 (2022).
[176] B. A. Bernevig, C. Felser, and H. Beidenkopf, "Progress and prospects in magnetic topological materials," Nature **603**, 41–51 (2022).
[177] X.-L. Qi, R. Li, J. Zang, and S.-C. Zhang, "Inducing a magnetic monopole with topological surface states," Science **323**, 1184–1187 (2009).
[178] Q. L. He, L. Pan, A. L. Stern, E. C. Burks, X. Che, G. Yin, J. Wang, B. Lian, Q. Zhou, E. S. Choi, K. Murata, X. Kou, Z. Chen, T. Nie, Q. Shao, Y. Fan, S.-C. Zhang, K. Liu, J. Xia, and K. L. Wang, "Chiral Majorana fermion modes in a quantum anomalous Hall insulator–superconductor structure," Science **357**, 294–299 (2017).
[179] M. Kayyalha, D. Xiao, R. Zhang, J. Shin, J. Jiang, F. Wang, Y.-F. Zhao, R. Xiao, L. Zhang, K. M. Fijalkowski, P. Mandal, M. Winnerlein, C. Gould, Q. Li, L. W. Molenkamp, M. H. W. Chan, N. Samarth, and C.-Z. Chang, "Absence of evidence for chiral Majorana modes in quantum anomalous Hall-superconductor devices," Science **367**, 64–67 (2020).

[180] W. Poirier and F. Schopfer, "Resistance metrology based on the quantum Hall effect," Eur. Phys. J.: Spec. Top. **172**, 207–245 (2009).
[181] X. Zhang and S.-C. Zhang, "Chiral interconnects based on topological insulators," Proc. SPIE **8373**, 837309 (2012).
[182] B. Lian, X.-Q. Sun, A. Vaezi, X.-L. Qi, and S.-C. Zhang, "Topological quantum computation based on chiral Majorana fermions," Proc. Natl. Acad. Sci. U. S. A. **115**, 10938–10942 (2018).
[183] K. M. Fijalkowski, N. Liu, P. Mandal, S. Schreyeck, K. Brunner, C. Gould, and L. W. Molenkamp, "Quantum anomalous Hall edge channels survive up to the Curie temperature," Nat. Commun. **12**, 5599 (2021).
[184] S. K. Kushwaha, I. Pletikosić, T. Liang, A. Gyenis, S. H. Lapidus, Y. Tian, H. Zhao, K. S. Burch, J. Lin, W. Wang, H. Ji, A. V. Fedorov, A. Yazdani, N. P. Ong, T. Valla, and R. J. Cava, "Sn-doped $Bi_{1.1}Sb_{0.9}Te_2S$ bulk crystal topological insulator with excellent properties," Nat. Commun. **7**, 11456 (2016).
[185] M. G. Vergniory, B. J. Wieder, L. Elcoro, S. S. P. Parkin, C. Felser, B. A. Bernevig, and N. Regnault, "All topological bands of all nonmagnetic stoichiometric materials," Science **376**, eabg9094 (2022).
[186] M. Dc, R. Grassi, J.-Y. Chen, M. Jamali, D. Reifsnyder Hickey, D. Zhang, Z. Zhao, H. Li, P. Quarterman, Y. Lv, M. Li, A. Manchon, K. A. Mkhoyan, T. Low, and J.-P. Wang, "Room-temperature high spin–orbit torque due to quantum confinement in sputtered $Bi_xSe_{(1-x)}$ films," Nat. Mater. **17**, 800–807 (2018).
[187] X. Liu, H.-C. Hsu, and C.-X. Liu, "In-plane magnetization-induced quantum anomalous Hall effect," Phys. Rev. Lett. **111**, 086802 (2013).
[188] P.-J. Guo, Z.-X. Liu, and Z.-Y. Lu, "Quantum anomalous Hall effect in antiferromagnetism," arXiv:2205.06702 (2022).
[189] C. N. Lau, M. W. Bockrath, K. F. Mak, and F. Zhang, "Reproducibility in the fabrication and physics of moiré materials," Nature **602**, 41–50 (2022).